

DTIC FILE COPY

FORMATION OF MONOLAYER FILMS BY THE SPONTANEOUS ASSEMBLY OF
ORGANIC THIOLS FROM SOLUTION ONTO GOLD

Colin D. Bain, E. Barry Troughton, Yu-Tai Tao,
Joseph Evall, George M. Whitesides*
Department of Chemistry
Harvard University
Cambridge MA 02138

Ralph G. Nuzzo
A.T. & T. Bell Laboratories
Murray Hill, NJ 07974

Technical Report No. 8 (September 1988)

Interim Technical Report

(Accepted for publication in J. Am. Chem. Soc.)

DISTRIBUTION STATEMENT A

Approved for public release
Distribution Unlimited

PREPARED FOR DEFENSE ADVANCED RESEARCH PROJECTS AGENCY
1400 Wilson Boulevard
Arlington VA 22209

DEPARTMENT OF THE NAVY
Office of Naval Research, Code 1130P
800 North Quincy Street
Arlington VA 22217-5000

ARPA Order No.: NR 356-856
Contract No.: N00014-85-K-0898
Effective Date: 85 September 01
Expiration Date: 88 August 31

Principal Investigator: George M. Whitesides
(617) 495-9430

The views and conclusions in this document are those of the authors and should not be interpreted as necessarily representing the official policies, either expressed or implied, of the Defense Advanced Research Projects Agency or the U.S. Government.

%0AAAAA803890595

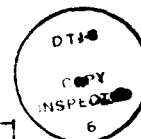
REPORT DOCUMENTATION PAGE

1. REPORT SECURITY CLASSIFICATION Unclassified			1b. RESTRICTIVE MARKINGS		
2. SECURITY CLASSIFICATION AUTHORITY			3. DISTRIBUTION / AVAILABILITY OF REPORT Approved for public release; distribution unlimited		
4. DECLASSIFICATION / DOWNGRADING SCHEDULE					
5. PERFORMING ORGANIZATION REPORT NUMBER(S) Technical Report #8			5. MONITORING ORGANIZATION REPORT NUMBER(S)		
6a. NAME OF PERFORMING ORGANIZATION Harvard University		6b. OFFICE SYMBOL (If applicable)		7a. NAME OF MONITORING ORGANIZATION Office of Naval Research	
7. ADDRESS (City, State, and ZIP Code) Office of Sponsored Research Holyoke Center, Fourth Floor Cambridge MA 02138-4993		7b. ADDRESS (City, State, and ZIP Code) Code 1130P 800 North Quincy Street Arlington VA 22217-5000			
8a. NAME OF FUNDING / SPONSORING ORGANIZATION ONR/DARPA		8b. OFFICE SYMBOL (If applicable)		9. PROCUREMENT INSTRUMENT IDENTIFICATION NUMBER	
9. ADDRESS (City, State, and ZIP Code) 800 North Quincy Street Arlington VA 22217-5000		10. SOURCE OF FUNDING NUMBERS			
		PROGRAM ELEMENT NO. 85-K-0898		PROJECT NO. NR 356-856	
		TASK NO.		WORK UNIT ACCESSION NO.	
11. TITLE (Include Security Classification) "Formation of Monolayer Films by the Spontaneous Assembly of Organic Thiols from Solution onto Gold"					
12. PERSONAL AUTHOR(S) Colin D. Bain, E. Barry Troughton, Yu-Tai Tao, Joseph Evall, George M. Whitesides*, Ralph G. Nuzzo					
13a. TYPE OF REPORT Interim		13b. TIME COVERED FROM TO		14. DATE OF REPORT (Year, Month, Day) September 1988	
15. PAGE COUNT					
16. SUPPLEMENTARY NOTATION					
17. COSATI CODES			18. SUBJECT TERMS (Continue on reverse if necessary and identify by block number)		
FIELD	GROUP	SUB-GROUP	monolayers alkanethiols gold wetting		
			XPS desorption ellipsometry		
19. ABSTRACT (Continue on reverse if necessary and identify by block number)					
<p>Long-chain alkanethiols, $\text{HS}(\text{CH}_2)_n\text{X}$, adsorb from solution onto gold surfaces and form ordered, oriented monolayer films. The properties of the interfaces between the films and liquids are largely independent of chain length when $n > 10$; in particular, wetting is not directly influenced by the proximity of the underlying gold substrate. The specific interaction of gold with sulfur and other "soft" nucleophiles and its low reactivity toward most "hard" acids and bases make it possible to vary the structure of the terminal group, X, widely and thus permit the introduction of a great range of functional groups into a surface. Studies of wettability of these monolayers, and of their composition using X-ray photoelectron spectroscopy (XPS), indicate that the monolayers are oriented with the tail group, X, exposed at the monolayer-air or monolayer-liquid interface. The adsorption of simple n-alkanethiols generates</p>					
20. DISTRIBUTION / AVAILABILITY OF ABSTRACT <input checked="" type="checkbox"/> UNCLASSIFIED/UNLIMITED <input type="checkbox"/> SAME AS RPT. <input type="checkbox"/> OTIC USERS			21. ABSTRACT SECURITY CLASSIFICATION		
22a. NAME OF RESPONSIBLE INDIVIDUAL Dr. Joanne Milliken			22b. TELEPHONE (Include Area Code)		22c. OFFICE SYMBOL

19. Abstract (cont'd)

hydrophobic surfaces whose free energy (19 mJ/m^2) is the lowest of any hydrocarbon surface studied to date. In contrast, alcohol and carboxylic acid-terminated thiols generate hydrophilic surfaces that are wet by water. Measurement of contact angles is a useful tool for studying the structure and chemistry of the outermost few angstroms of a surface. This work used contact angles and optical ellipsometry to study the kinetics of adsorption of monolayer films and to examine the experimental conditions necessary for the formation of high-quality films. Monolayers of thiols on gold appear to be stable indefinitely at room temperature but their constituents desorb when heated to 80°C in hexadecane. Long-chain thiols form films that are thermally more stable than films formed from short-chain thiols.

Accession For	
NTIS	CRA&I <input checked="" type="checkbox"/>
DTIC	TAB <input type="checkbox"/>
Unannounced	<input type="checkbox"/>
Justification	
By	
Distribution /	
Availability Codes	
Dist	Available and/or Special
A-1	



JA8808691

REVISED

Formation of Monolayer Films by the Spontaneous Assembly of
Organic Thiols from Solution onto Gold¹

Colin D. Bain,² E. Barry Troughton, Yu-Tai Tao, Joseph Evall,
George M. Whitesides*

Department of Chemistry,

Harvard University,

Cambridge, MA 02138

Ralph G. Nuzzo

A.T. & T. Bell Laboratories,

Murray Hill, NJ 07974

Abstract. Long-chain alkanethiols, $\text{HS}(\text{CH}_2)_n\text{X}$, adsorb from solution onto gold surfaces and form ordered, oriented monolayer films. The properties of the interfaces between the films and liquids are largely independent of chain length when $n > 10$; in particular, wetting is not directly influenced by the proximity of the underlying gold substrate. The specific interaction of gold with sulfur and other "soft" nucleophiles and its low reactivity toward most "hard" acids and bases make it possible to vary the structure of the terminal group, X, widely and thus permit the introduction of a great range of functional groups into a surface. Studies of wettability of these monolayers, and of their composition using X-ray photoelectron spectroscopy (XPS), indicate that the monolayers are oriented with the tail group, X, exposed at the monolayer-air or monolayer-liquid interface. The adsorption of simple n-alkanethiols generates hydrophobic surfaces whose free energy (19 mJ/m^2) is the lowest of any hydrocarbon surface studied to date. In contrast, alcohol and carboxylic acid-terminated thiols generate hydrophilic surfaces that are wet by water. Measurement of contact angles is a useful tool for studying the structure and chemistry of the outermost few angstroms of a surface. This work used contact angles and optical ellipsometry to study the kinetics of adsorption of monolayer films and to examine the experimental conditions necessary for the formation of high-quality films. Monolayers of thiols on gold appear to be stable indefinitely at room temperature but their constituents desorb when heated to 80

°C in hexadecane. Long-chain thiols form films that are thermally more stable than films formed from short-chain thiols.

Introduction

This paper describes studies on the preparation and characterization of well-ordered monolayer films formed by the adsorption of long-chain alkanethiols ($\text{HS}(\text{CH}_2)_n\text{X}$) from solution onto the surface of gold. This work is part of a program of physical-organic chemistry intended to explore the relationships between the microscopic structure of organic surfaces and their macroscopic properties (especially wettability). Studies of organic monolayer films have focussed on two distinct methods of preparation: Langmuir-Blodgett techniques,^{3,4} involving the transfer of a film assembled at an air-water interface to a solid substrate, and self-assembly, based on the spontaneous adsorption of the film components from a solution directly onto the substrate.^{5,6} Interest in self-assembled monolayers has focussed on a number of systems including chlorosilanes on silicon,⁷ carboxylic acids on metal oxides,⁸ and organosulfur compounds on gold.^{9,11-18} The work described in this paper lies in the last system because these monolayers offer the best presently available combination of high structural order, flexibility in the structure of functional groups exposed at the solid-vapor or solid-liquid interface, and ease of preparation and analysis.

Organosulfur derivatives coordinate strongly to many metal and metal sulfide surfaces and form monomolecular films; the widespread use of xanthates in ore flotation¹⁰ provides a historically important application of this phenomenon. In 1983,

Nuzzo and Allara¹¹ showed that dialkyl disulfides formed oriented monolayers on gold. Since then, several other studies have characterized aspects of these monolayers,¹²⁻¹⁴ demonstrated the use of self-assembled monolayers as electrochemical barriers,¹⁵ and extended the technique to the adsorption of proteins¹⁶ and phospholipids.¹⁷ Porter et al.¹⁸ have presented data on monolayers of alkanethiols adsorbed on gold, using optical ellipsometry, infrared spectroscopy and electrochemistry to characterize the monolayers. The work reported in this paper is a complementary effort that has proceeded simultaneously and in close collaboration with the spectroscopic efforts of Porter et al., and has focussed on the experimental conditions needed to obtain high-quality monolayers, on the wetting properties of the monolayers, and on the use of X-ray photoelectron spectroscopy in characterizing the monolayer films. In subsequent papers we will address the preparation of polyfunctional surfaces and multi-component monolayers, and the use of these systems in studying wetting, chemical reactivity, adhesion and tribology at solid-liquid and solid-vapor interfaces.

The utility of thiols adsorbed on gold as a monolayer system is based on three considerations. First, gold is a relatively inert metal: it does not form a stable oxide surface¹⁹ and it resists atmospheric contamination. Second, gold has a strong specific interaction with sulfur¹³ that allows us to form monolayers in the presence of many other functional groups.^{20,21} Third, long-chain alkanethiols form a densely-packed, crystalline

or liquid-crystalline monolayer on gold.^{18,22}

We believe that the high degree of structural order in this system, combined with the ability to vary synthetically the three-dimensional chemical make-up in a pre-determined and well-defined way, will make thiols on gold a system of wide utility for studies in the physical, chemical and biological sciences.

Results and Discussion

General Procedure. We prepared oriented organic monolayers by immersing thin ($\sim 2000 \text{ \AA}$), evaporated, gold films in dilute solutions of alkanethiols. Typical experimental conditions used in forming a monolayer involved immersing a gold-coated silicon slide (ca. 1 X 3 cm, cut from a 3-in. wafer) in a 1 mM solution of the alkanethiol overnight at room temperature. The strong specific interaction between the sulfur atom and the gold surface induces the spontaneous assembly of an adsorbed monolayer at the gold-solution interface. The alkanethiols used in these experiments were pure by NMR spectroscopy and TLC, but we did not have to take exceptional efforts to obtain very high purities in order to obtain reproducible results.

We controlled the chemical functionality at the surface by varying the tail group, X, of the adsorbate, $\text{HS}(\text{CH}_2)_n\text{X}$. Essentially any functional group that is compatible with the thiol may be introduced at the surface in this manner, although large tail groups may interfere with the packing of the hydrocarbon chains. In all the cases that we have examined, coordination of the thiol to the gold was strongly preferred over binding through the tail group and there is no ambiguity concerning the regiochemistry of the adsorption.²³ We used optical ellipsometry, contact angle measurement and X-ray photoelectron spectroscopy (XPS) to characterize the monolayers and confirm the presence of the expected functional groups at the monolayer-air or monolayer-

liquid interface.

Measurement and Interpretation of Contact Angles. To avoid confusion we will use the following nomenclature in this and subsequent papers to define the contact angle, θ . The subscript "a" or "r" after θ denotes advancing or receding angles, respectively. The superscript after θ denotes the ambient medium surrounding the surface. Where no medium is specified the measurements were made under air saturated with the liquid used for the contact angle measurement.²⁴ This liquid is specified in parentheses after θ . Thus $\theta_a(\text{HD})$ denotes the advancing contact angles of hexadecane under air. Our use of the term "wets" also requires some clarification. We have never observed a single 1- μl drop to spread over an entire slide even when other data indicated that the spreading coefficient²⁵ should have been positive. Consequently, we have adopted the operational, though somewhat arbitrary, definition of wetting as an irregular drop shape and a contact angle of less than 10° . We will show in this paper that the surface of the monolayer is composed largely, if not exclusively, of the tail groups of the thiols adsorbed on gold. We will thus use terms such as "methyl surface" when referring to a monolayer as shorthand for the phrase "surface of a monolayer in which the terminal group of the alkyl chain is a methyl group". We will also use the terms "monolayer of alkanethiol" and "monolayer of disulfide" to specify the precursor from which the monolayer was derived. In both cases the probable species on the surface is a gold thiolate,

RS⁻Au(I).¹²

Interpretation of contact angles and comparison of contact angles on different surfaces (or even on the same surface by different investigators) are complicated by two factors. First, a surface rarely exhibits a unique, thermodynamic, equilibrium contact angle²⁶ as defined by Young's equation;²⁷ hysteresis is observed. Readings depend on whether the drop has advanced or receded across the surface prior to measurement. In previous studies this hysteresis has been greatest for polar,²⁸ heterogeneous,^{29,30,31,32,33} or rough^{34,35,36} surfaces and for polar contacting liquids, and least for smooth,³⁷ uniform, non-polar surfaces and for non-polar liquids. We observe some hysteresis on most of the monolayers that are not wet by the contacting liquid. The hysteresis, where $\cos\theta_{r,min} - \cos\theta_{a,max}$ is in the range 0.1 to 0.15, is relatively small and is not strongly correlated with the polarity of the tail group. Hysteresis appears to be greater on contaminated surfaces and on monolayers in which a polar group is "buried" beneath the surface.⁹ Most of the contact angles reported in this paper are advancing angles.

To compound difficulties in interpretation, the measured advancing contact angle varies with how the reading is made. The maximum advancing contact angle, as defined by Dettre and Johnson,³⁰ is the angle observed in the limit that the drop is advanced quasistatically over a motionless surface (referred to as Method B in this paper).³⁸ Under these conditions the drop

has no internal energy to surmount any small kinetic barriers that may hinder its advance. In practice, vibrations and the finite speed with which the drop is advanced over the surface result in an observed angle somewhere between the maximum advancing contact angle and the equilibrium contact angle (if such a quantity actually exists^{39,40}).

An alternative procedure (Method A), which we have employed extensively, yields somewhat lower angles but has the advantage of greater reproducibility. A drop of a fixed size is formed on the end of a hydrophobic needle and lowered to the surface. As the needle is raised, the drop detaches itself from the tip and advances across the surface. The kinetic energy of the drop allows it to surmount small energy barriers that might not be overcome by vibrational perturbation alone. For water on a methyl surface Method A yields contact angles about 2° lower than Method B. For hexadecane we observed no significant difference in the contact angles.

We feel that until it is clear how measured contact angles are related to equilibrium and thermodynamic angles, it is important to employ a technique that facilitates comparison of data obtained on different systems and in different laboratories. Thus, we used Method A to obtain most of the data quoted in this paper.

A second factor that complicates comparisons is the effect of the roughness of the surface on the measured contact angle and the relationship of the measured to the true contact angle for

the surface. Simple thermodynamic arguments⁴¹ predict that on a chemically homogeneous surface with roughness factor, r ,⁴² the observed angle, θ , is related to the true angle, θ_{true} , on a smooth surface by eq 1.

$$\cos\theta = r\cos\theta_{\text{true}} \quad (1)$$

Consequently, in the absence of metastable states, roughness should increase angles that are greater than 90° and decrease those that are less than 90° . Other investigators^{34,43,44} have observed that upon roughening a smooth non-polar surface the advancing contact angle increased, the receding angle decreased, and, as a consequence, the hysteresis increased. As the surfaces were made progressively smoother, both the advancing angle and the hysteresis decreased. No hysteresis was observed on extremely smooth paraffin wax.³⁷ For surfaces exhibiting large hysteresis, the arithmetic mean of θ_a and θ_r has sometimes been reported (see Table II) although this number has no clear significance.

We have employed gold films deposited in several different thermal and electron-beam evaporators; the contact angles always lay within a three-degree range although the gold surfaces were certainly of different roughness on a length scale of 100 \AA . A monolayer of octadecanethiol was adsorbed on a gold film evaporated onto the unpolished side of a silicon wafer. The morphology of the surface was very rough, consisting of $10\text{-}\mu\text{m}$ pyramidal asperities. The advancing contact angles of water and

hexadecane on this surface were not significantly different from monolayers on smooth gold, although the hysteresis was about twice as great.

Properties of Monolayer Films Formed from n-Alkanethiols as a Function of Chain Length. We examined the effects on the properties of monolayers of varying the chain length, n , in the homologous series of n-alkanethiols, $\text{CH}_3(\text{CH}_2)_n\text{SH}$, using ellipsometric and contact angle measurements. Figure 1 shows a plot of the ellipsometric thickness against n . The data are reasonably described by a straight line with a slope of 1.5 Å per CH_2 and a y-intercept of -1.9 Å. Also shown, as a dotted line, is the thickness predicted for a fully extended, all-trans configuration oriented normal to the surface. Using known bond lengths and bond angles,^{45,46} and assuming binding to the surface via a thiolate moiety, we estimated a theoretical slope of 1.27 Å per CH_2 unit and an intercept of 4 Å. The dashed line represents the thickness expected for a monolayer tilted 30° (the mean tilt inferred from reflectance infrared spectra^{18,47}) from the normal to the surface.

Two aspects of the experimental data require comment: the negative intercept and the steep slope. In interpreting the ellipsometric data, we note that the measured quantity is the difference between the thickness of the adsorbed material on the monolayer-coated gold and on an ostensibly clean gold surface.⁴⁸ Although gold is inert, compared with most other metals, towards chemisorption of O_2 , CO , H_2O , and hydrocarbons,⁴⁹⁻⁵¹ the

surface is nevertheless of high free energy and, under ambient laboratory conditions, covered with a reversibly physisorbed layer of water, hydrocarbons, and other organic compounds.^{51,52} Adsorption studies on other high-energy metallic and non-metallic surfaces⁵³⁻⁵⁶ indicate the presence of several angstroms of water when the relative humidity is in the ambient range (20 - 80%). Furthermore, within minutes of exposure to the laboratory atmosphere,⁵⁵⁻⁵⁸ a clean, hydrophilic,⁵⁹ gold surface is rendered hydrophobic by adsorption of non-polar contaminants. Our slides typically exhibited contact angles in the range $\theta_a(\text{H}_2\text{O}) = 30-70^\circ$ before immersion in the thiol solutions. XPS indicates the presence of about 6 Å of non-volatile carbon and oxygen-containing contaminants on our "clean" gold surfaces.⁶⁰ In contrast, the methyl surface generated by adsorption of a long-chain alkanethiol is of much lower free energy, and hence less prone to physisorption of overlayers and less susceptible to contamination. Comparable low energy surfaces reversibly adsorb less than 2 Å of water at ambient humidities^{56,61-63} and show little evidence of irreversible contamination of the surface.^{64,65} Consequently, more adventitious material is present on (and subsequently displaced from) the bare gold surface than on the monolayer. This difference leads to observed thicknesses that are less than the true thicknesses and is of approximately the correct magnitude to account for the discrepancy between experiment and prediction. The size of this effect will vary from laboratory to laboratory and even from day

to day and is, in our opinion, a major contributor to the observed scatter in the ellipsometric data. It may also be partially responsible for differences in results between investigators.

The observed slope of 1.5 Å per methylene is in exact agreement with that obtained by Porter et al.¹⁸ for chains with $n > 10$. It is, however, significantly greater than the value predicted for chains oriented normal to the surface. The discrepancy is even greater if the chains are tilted 30° relative to the normal as inferred from infrared data.^{18,47} One possible explanation is that longer chains, even for $n > 10$, are more densely packed, but infrared, XPS⁶⁶ and contact angle measurements provide no support for this hypothesis. Part of the discrepancy between the observed and calculated slopes may arise from our use of a constant refractive index, independent of chain length: the additional close-packed methylenes may have a refractive index comparable to polyethylene ($n \sim 1.5$), rather than the value of 1.45 used in the reduction of the ellipsometric data. A rigorous analysis would also take account of the tensor nature of the refractive index and use elements of n averaged over the molecular orientations within the film. Another possible explanation is our assumption of a plane, parallel model for the monolayers on gold even though the surface is not rigorously flat. We expect that roughness would result in a systematic error in the calculated film thickness across the series of alkanethiols, although the effect of roughness on a

scale of a few hundred angstroms on the ellipsometric constants is not clear.⁶⁷

For short chains ($n < 8$) Porter noted a marked drop-off in the ellipsometric thicknesses, implying loose packing, concomitant with infrared data indicating increasing disorder. Although an abrupt change in structure is not evident from our ellipsometric studies, we see a similar trend in the contact-angle data (Figure I). For $n > 10$, advancing contact angles $\theta^{\text{air}}(\text{H}_2\text{O}) = 111 - 114^\circ$ and $\theta^{\text{air}}(\text{HD}) = 45^\circ - 48^\circ$ were consistently observed; for shorter chains the contact angles were progressively lower. This trend could be due either to the probe liquid sensing the underlying gold⁶⁸ or to increasing disorder in short-chain monolayers exposing methylene groups at the surface: we have observed low contact angles in partially formed monolayers and in monolayers where disorder has been introduced intentionally at the surface.²⁰ In a previous study of adsorption of *n*-alkanoic acids on oxidized aluminum, Allara and Nuzzo⁸ also observed changes in properties of shorter monolayers: for $n < 11$, ellipsometric thicknesses were widely scattered and for $n < 14$ a drop-off in the contact angles was evident. The contact angles in this region exhibited a marked odd-even variation with chain length. The contact angles with hexadecane suggest that a similar, though less pronounced, effect may occur with thiols on gold, particularly for short ($n < 11$) chains. Our principal interest here lies in the longer-chain thiols where the properties of the monolayers are largely independent of chain

length.

We also studied carboxylic acid-terminated thiols of varying chain lengths (Figure 2). The ellipsometric thicknesses lie on a good straight line with a slope of 1.16 Å per methylene unit and a y-intercept of 4.8 Å. The dotted line (intercept 5 Å, slope = 1.27 Å/CH₂) and dashed line represent the calculated thicknesses as before. The observed and calculated intercepts agree almost exactly, in contrast to the methyl-terminated case. The carboxylic acids generate a high-energy surface (the monolayers are wet by water and hexadecane for all chain lengths) which, like gold, contaminates rapidly in the laboratory atmosphere. We demonstrated explicitly the differing susceptibility of methyl and acid surfaces to contamination by exposing monolayers of 16-mercaptohexadecanoic acid and docosanethiol on gold to the vapor above an opened bottle of octylamine for ten seconds. The thickness of the organic surface layer in the former case increased by 7 Å and the contact angle with water rose to 60° (reflecting adsorption of a partial monolayer of the amine on the acid surface). The methyl-terminated monolayer surface was unaffected. It is probable that significant amounts of water are adsorbed at the acid-air interface; polymer surfaces of lower polarity (polycarbonate, PMMA) adsorb at least a monolayer at ambient humidities.^{56,69} In fact, near 100% relative humidity, it is thermodynamically favorable for a macroscopic film of water to condense onto the acid surface; a drop of hexadecane beads on a film of HS(CH₂)₁₅CO₂H at 100% relative humidity as though on

the surface of a beaker of water.⁷⁰ It is possible that the adventitiously adsorbed material before and after monolayer formation are of comparable thickness and their influence on the ellipsometric thickness cancels.

The observed slope of 1.16 Å per CH₂ group is consistent with the mean tilt of 25° in the hydrocarbon chains deduced for methyl-terminated thiols from infrared spectra.^{18,47} This agreement is surprising since many of the effects that might have caused deviations in the slope of the ellipsometric data in Figure 1 should also have influenced those in Figure 2. Furthermore, infrared spectra of the carboxylic acid and methyl-terminated monolayers show only subtle differences in the C-H stretching region. No gross structural changes, which might be responsible for the different slopes in the ellipsometric data, appear to be induced by hydrogen-bonding between the carboxylic acids. At present, we do not understand the differences in the ellipsometric behavior of the methyl and acid-terminated monolayers.

Wetting Properties of Monolayers of Alkanethiols. The ability to modify the tail group of the thiol adsorbates allows us to vary the wetting properties of the monolayer extensively. Competitive adsorption of two or more thiols permits even greater flexibility in the specification of surface wettability.⁷¹ Many different functional groups can be introduced at the surface subject only to the three constraints that (a) they do not compete strongly with the thiol as a head group for coordination

to the gold; (b) they do not react with thiols; and (c) they are not so large as to prevent close-packing of the hydrocarbon chains. This last point may be illustrated by the monolayer formed from 11-(*t*-butyldimethylsiloxy)-1-undecanethiol, a molecule with a club-like tail group (Table I). The contact angles are significantly lower than expected for a methyl surface (Table II) and indicate a disordered surface. Cleavage of the silyl protecting group with F^- (leaving a hydroxyl group) yielded a monolayer with the properties expected ($\theta_a(H_2O) = 52^\circ$, $\theta_a(HD) = 0^\circ$) for a surface composed of a 1:1 mixture of alcohol and methyl or methylene groups.²⁰ External reflection infrared spectra⁴⁷ of monolayers of 16-carbon thiols terminated by carboxylic acid, alcohol, ester, ether or amide groups showed remarkably little variation in the tilt and packing of the polymethylene chains. As the length of the hydrocarbon chain becomes shorter the perturbations of the structure of the monolayer by interactions between the tail groups increase.

Table I summarizes the contact angles of water and hexadecane on representative monolayers. We have prepared surfaces that span the whole range of $\theta_a(H_2O)$ from close to zero for highly polar functional groups such as carboxylic acids and alcohols (as predicted by Adam⁷²) to 118° for a surface exposing CF_3 groups. Even higher angles would probably be observed if longer telomers could be obtained in high purity.⁷³ Hexadecane wets any surface in which the outermost group is polar, but it exhibits angles of over 70° on a fluorinated surface. A

comparison of the nitrile and methyl ester surfaces provides an interesting example of the length scales determining the wetting interaction.⁷⁴ Both surfaces have comparable contact angles with water, but hexadecane only wets the nitrile surface. On the methyl ester surface, the hexadecane interacts primarily by a London force with the exposed methyl group, whereas the water senses the underlying polar ester functionality, either by penetration into the monolayer or possibly as a result of fixed dipole-dipole interactions having a longer range than dispersion forces.⁷⁵ An alternative explanation--that the surface reconstructs to expose the polar ester group at the monolayer-water interface--cannot be ruled out.⁷⁶

The contact angles are consistent with our notion that the thiols adsorb approximately perpendicular to the gold surface and are sufficiently densely packed to expose the tail group at the surface. There is no evidence in monolayers of simple long-chain thiols (unlike dialkyl sulfide monolayers⁹) of intramonolayer disorder, surface reconstruction, or burying of polar functional groups within the interior of the monolayer. The observed angles are stable, reproducible, and where more than one chain length has been synthesized, largely independent of chain length (see above).

Surfaces Composed of Methyl Groups. The contact angle of water on a smooth surface composed of methyl or methylene groups has been the subject of numerous previous studies (Table II). Table II distinguishes several different experimental methods of

measuring contact angles: "max" indicates a maximum advancing angle obtained by the method of Dettre and Johnson³⁰ or some equivalent technique; "eq" refers to drops that have in some way been equilibrated to allow them to overcome small kinetic barriers that may hinder their advance; and "mean" is the arithmetic average of the maximum advancing and minimum receding contact angles, a value that has often been quoted but whose significance is unclear.

In general, surfaces composed of methyl groups exhibit higher contact angles than those exposing methylene groups. Methyl groups do not generate a lower-energy surface because they are intrinsically less polarizable than methylene groups; in fact methyl groups are significantly more polarizable, and even after compensating for the differing molar volumes the polarizabilities are comparable.⁷⁷ An alternative explanation is that a close-packed methyl surface maximizes lateral van der Waals interactions, minimizes the exposed molecular surface area, and thus minimizes the additional interactions between the monolayer and a supernatant liquid. As the methyl groups at the interface become less closely-packed the number of exposed methylene groups increases and lateral dispersion interactions decrease. Consequently the surface free energy increases and the contact angles decline.

Despite the difficulties in comparing contact angles on different surfaces (vide supra), we believe that the "true" value of the contact angle of water on a surface composed of the

terminal methyl groups of hydrocarbon chains probably lies in the range 110-115°, with the exact value depending on the packing and orientation of the methyl groups at the interface. Our thiol monolayers exhibit contact angles of 111-115°. Comparison of the contact angles of hexadecane and bicyclohexyl with previous measurements (Table II) also suggests a well-packed methyl surface. Some hysteresis in the contact angle is observed, even though scanning electron microscopy indicates that the surface roughness (Figure 3)¹³ is on a scale of only a few hundred angstroms--well below the length scale expected theoretically to give rise to hysteresis.^{31,78}

Figure 4 plots contact angles on a monolayer of docosane-thiol on gold of various liquids against the surface tension, γ_{lv} , of the liquid (a Zisman plot^{6,79}). A quadratic (the dotted line in Figure 4) fits the data for hydrocarbon liquids well; cyclohexane is the only liquid that yields an angle that does not fall on the line. Both the quadratic fit and the more normal linear extrapolation yield a critical surface tension $\gamma_c = 19$ mN/m for this surface.⁸⁰ If the interactions in both the monolayer and the contacting liquid are purely dispersive then, using a geometrical mean approximation for the solid-liquid interfacial tension, γ_{sl} ,⁸¹ $1 + \cos \theta = 2(\gamma_{sv}/\gamma_{lv})^{1/2}$. When $\cos \theta$ is plotted against $(\gamma_{lv})^{-1/2}$ the data for alkanes and other hydrocarbons (with the exception of cyclohexane) fall on a straight line with correlation coefficient of 1.00 and a slope that yields a value for the solid-vapor interfacial tension, γ_{sv}

= 19.3 ± 0.6 mN/m. The contact angles with alcohols are uniformly higher than with alkanes with the same surface tensions.^{74,82} The value of γ_c obtained from the data with alcohols is very sensitive to the extrapolation chosen.

Table III shows an assortment of literature values for comparison. The critical surface tension is significantly lower than for single crystals of n-hexatriacontane or monolayers of octadecylamine on chromium, but still higher than for perfluorinated surfaces.⁸³

Effect of Contamination by Disulfides. Nuzzo and Allara^{11,13} have shown that dialkyl disulfides, like thiols, adsorb onto a gold surface and form oriented monolayers. Although our thiols are free (<1% impurity) from contamination by disulfides by NMR spectroscopy, the latter are certainly present to some extent. Furthermore, experiments are not conducted under anaerobic conditions so we expect some oxidation to disulfides after the solutions used in the adsorptions have been prepared. To determine the extent of this oxidation, we analyzed by NMR spectroscopy a two-week-old, 4 mM solution of $\text{HS}(\text{CH}_2)_{10}\text{CO}_2\text{H}$ prepared in degassed ethanol: no ester was detected, but about 3% of the disulfide was observed. At higher dilutions, or if slides are repeatedly removed from and immersed into the solution, the proportion of disulfide is likely to be even higher. For this reason, we generally employed freshly prepared solutions.

The monolayers generated from pure thiols and from the corresponding disulfides are similar in many ways,²² but we have

not shown unambiguously that they are indistinguishable. It is therefore important to demonstrate that low levels of disulfides present as impurities in solutions of thiols do not adsorb preferentially onto the gold surface. We have used competitive adsorption experiments to eliminate this possibility (Figure 5).

We performed two adsorption experiments: in the first experiment we prepared a series of solutions of varying concentrations of $\text{HS}(\text{CH}_2)_{11}\text{OH}$ and $[\text{S}(\text{CH}_2)_{10}\text{CH}_3]_2$ with the total concentration of sulfur-- $[\text{RSH}] + 2[\text{R}_2\text{S}_2]$ --held constant at 1 mM. The disulfide was counted at twice its actual concentration because each molecule contributes two chains to the monolayer. To eliminate any influence of the tail group on the kinetics or thermodynamics of adsorption we performed a second experiment using solutions containing mixtures of the methyl-terminated thiol ($\text{HS}(\text{CH}_2)_{10}\text{CH}_3$) and the alcohol-terminated disulfide ($[\text{S}(\text{CH}_2)_{11}\text{OH}]_2$). Since a highly organized surface composed of alcohol groups yields a very low contact angle with water and a surface composed of methyl groups a high one, the contact angle provides a sensitive and convenient measure of which species has been adsorbed at the surface. Figures 5(b) and 5(c) suggest a strong preference for adsorption of the thiol in both experiments. The curvature in the graphs of contact angle against composition implies that some disulfide is adsorbed in the presence of thiol, but the preference for adsorption of the thiol relative to the disulfide is at least 10:1. Trace contamination of solutions of alkanethiols by dialkyl disulfides is thus

unlikely to affect our results. These observations are qualitative: quantitative studies on the competitive adsorption of thiols and disulfides will be published separately.

Two observations suggest that this preference for adsorption of thiols relative to the corresponding disulfides is principally a kinetic phenomenon. First, a solution of a thiol displaces a preformed monolayer (of either a thiol or a disulfide) faster than the corresponding disulfide does, but this rate is essentially independent of whether the monolayer was initially formed from a thiol or its disulfide.⁸⁴ Second, thermal desorption of monolayers of thiols adsorbed from solution and their corresponding disulfides occur at approximately the same rate.⁸⁵ These observations suggest that thiols and disulfides give rise to similar species⁸⁶ on the surface but that the kinetics of adsorption and displacement are different. We note that recent UHV studies of organosulfur compounds on Au (111)¹² suggest that the strongly chemisorbed state from either a thiol or disulfide is probably a surface thiolate ($\text{RS}^-\text{Au(I)}$).

Kinetics of Formation of Monolayers. The rate of formation of a self-assembled monolayer is influenced by many factors some of which can be controlled relatively easily, such as temperature, solvent, concentration and chain length of the adsorbate, and the cleanliness of the substrate, and others, such as the rate of reaction with the surface and the reversibility of adsorption of the components of the monolayer, that are inherent to the system. Experimental conditions must be established for

each new system studied; adsorption times varying from a few seconds for arachidic acid on ZnSe⁸⁷ to several days for n-alkanoic acids on aluminum⁸ have been employed. We have used ellipsometry and contact angle to investigate the effect of different chain lengths, tail groups, and concentrations on the kinetics of adsorption, and to explore the influence of the solvent on the character of the monolayers formed by adsorption of alkanethiols on gold.

At moderate concentrations (ca. 1 mM) the adsorption process is characterized by two distinct phases. Initial formation of the monolayer is rapid: a clean gold slide placed in a 1 mM solution of a long-chain alkanethiol in ethanol is autophobic⁸⁸ after about two seconds. Within a few minutes the contact angles are close to or have reached their limiting values and the thickness has risen to 80 - 90% of its maximum. This initial, rapid adsorption is followed by a slower period lasting several hours during which the thickness slowly approaches its final value. For 1 mM solutions of alkanethiols, we immersed the slides overnight to ensure that monolayer formation was complete.

This behavior can be rationalized by rapid adsorption of an imperfect monolayer followed by a slower process of additional adsorption and consolidation, possibly involving displacement of contaminants, expulsion of included solvent from the monolayer, and lateral diffusion on the surface to reduce defects and enhance packing. The incorporation of solvent into a self-assembled monolayer is well-known and is a particularly acute

problem when the solvent and the adsorbate are geometrically matched (e.g octadecylamine adsorbed from hexadecane).^{89,90} In general, the included solvent is expelled from the monolayer after a sufficiently long adsorption time;⁸⁹ in a few cases, incorporation of solvent was still observed after several days.^{90,91}

Figure 6 shows the kinetics of adsorption of octadecanethiol and decanethiol as 1 mM solutions in ethanol. Limiting properties were reached within 1000 minutes in both cases. The scatter in the data for longer times gives an indication of their precision. The contact angles on the decanethiol monolayer approach their limiting values more slowly than on the octadecanethiol monolayer for two reasons. First, the ten-carbon chain of decanethiol approaches the lower limit in chain length below which a decrease in the limiting contact angles was observed (Figure 1). Consequently, imperfections or loose packing in a monolayer comprised of short-chain thiols may have a greater effect on contact angles than will similar defects for longer chains. Second, hexadecane may penetrate into holes in the octadecanethiol monolayer, improve the packing of the chains, and increase the contact angle with hexadecane.⁹²

We have asserted earlier that thiols displace contaminants from the surface. We demonstrated this assertion explicitly by displacing a preformed monolayer of propanethiol on gold (as strongly adsorbed a contaminant as is routinely encountered in our laboratory) by octadecanethiol (Figure 7). The effect on the

kinetics of formation (as measured by the ellipsometric thickness) in the initial phase was marked but the limiting thickness was unaffected.

Shafrin and Zisman⁹³ observed that octadecylamine derivatives with highly dipolar tail groups, such as CF_3 , were adsorbed on platinum much more slowly than the methyl-terminated analogues. We observed no significant differences in the kinetics of adsorption of octadecanethiol and 16-mercaptohexadecanoic acid (Figure 8): the ellipsometric thickness of the acid-terminated thiol paralleled that of octadecanethiol and water wetted the monolayer after only three minutes. The initial increase in the contact angle arises from screening of the hydrophilic gold surface by the methylene chains in a disordered, partial monolayer.

We also used ellipsometry and contact angle of hexadecane to follow the kinetics of monolayer formation as a function of concentration. Under the experimental conditions used (1 cm x 3 cm slides, 20 mL of solution), one monolayer of material corresponds to a concentration of alkanethiol in solution of about 0.0001 mM. Figure 9 plots the adsorption kinetics over four decades of concentration, from 1 mM to 10^{-4} mM.⁹⁴ We note that at long adsorption times and at high dilutions the problem of conversion of the alkanethiol to disulfide may be acute. We have found that 1 mM is a convenient concentration for most experimental work, but if solubility or other considerations require it, dilutions of up to 10^{-2} mM can be used to form good

monolayers, given sufficient time for the adsorption to reach completion. At 10^{-3} mM only an imperfect monolayer had formed after one week, although formation of partial monolayers was still observed at much lower concentrations. The implication of our experimental observations at high dilution is that adsorbates and adsorption vessels must be scrupulously free of contaminating long-chain thiols if monolayers of high quality are to be obtained. A control slide exposed to pure ethanol containing no octadecanethiol showed no evidence of the adsorption of additional material.

Effect of Solvent on Monolayer Formation. Ethanol has been our preferred solvent on grounds of its low cost, low toxicity, low tendency to be incorporated into the monolayer, and availability in high purity. On occasion, reactivity, solubility, or other considerations may require the use of alternative solvents or even the alkanethiol as a neat liquid. To survey the suitability of other solvent systems, we placed gold slides in 1 mM solutions of hexadecanethiol in a range of solvents and in the neat liquid (Figure 10).

In all cases autophobic monolayers formed, but some solvents yielded monolayers with higher contact angles than others. The hexadecanethiol monolayers adsorbed from hexadecane had the expected thickness, but exhibited abnormally low contact angles, possibly due to the incorporation of hexadecane into the monolayer. We note that, when hexadecane is used as the adsorption solvent, we have had difficulty forming monolayers of

long-chain alcohol and carboxylic acid terminated thiols that are wet by water. The salient feature of the ellipsometric data is the anomalously high thickness of the monolayers adsorbed from the neat thiol. This behaviour is not purely an aberration since we observed similar results with tetradecanethiol;⁹⁵ we are currently at a loss for a satisfactory explanation.

Evidence Concerning the Structure of Monolayers from X-ray Photoelectron Spectroscopy (XPS). Ellipsometric and contact angle data support the formation of oriented, self-assembled monolayers at the gold surface. Additional confirmation is provided by XPS.⁹⁶

Figure 11 (left) shows survey spectra for six representative monolayers on gold. We did not need to cool the samples to below room temperature to minimize the consequences of beam-induced damage: the level of damage to the sample was insignificant in the acquisition times used. These spectra confirm the presence of the desired elements in the monolayer and allow us to calculate its atomic composition. Percentage atomic compositions derived from XPS have to be interpreted with great care since photoelectrons from the sub-surface atoms are attenuated by the overlying material.^{96,97} The calculated atomic composition is sensitive to the energy of the primary X-ray beam, variations in photo-ionization cross-section with chemical structure, the take-off angle, and the elemental distribution perpendicular to the surface, in addition to the actual composition of the monolayer. Elemental compositions obtained by XPS are useful nevertheless:

at worst, they indicate qualitatively the elements present in the monolayer; at best, they yield, through angular-dependent studies, a depth profile of the surface region. Table IV shows the atomic compositions derived from the survey spectra in Figure 11.⁹⁸ For all the monolayers studied, we observed the expected elements and no others. In these and other studies the calculated atomic composition has routinely overstated the proportion of the tail group in the monolayer and the sulfur signal has been very weak due to inelastic scattering of the S(2p) electrons by the molecules in the monolayer, consistent with our proposed model for the monolayer orientation.

We performed a qualitative angle-dependent study on a monolayer of $\text{HS}(\text{CH}_2)_{10}\text{CO}_2\text{CH}_3$ on gold to confirm that the ester group lay at the surface. As the take-off angle (the angle between the surface and the photoelectrons accepted by the analyzer) decreases the surface sensitivity of XPS increases.⁹⁹ Table V shows the atomic compositions derived from survey spectra at three take-off angles. As expected, the gold and sulfur intensities decreased and the carbon and oxygen intensities increased at lower take-off angles. Further, the ratio of carbon to oxygen decreased confirming that, on average, the oxygen atoms were nearer to the surface than the carbon atoms. More dramatic evidence is shown in Figure 12, which plots high resolution spectra of the carbon 1s region at take-off angles of 90° and 15°. In the grazing angle spectrum, the intensities of the two outermost carbons were enhanced by about 50% relative to the

carbons in the polymethylene chains.

The position of a photoelectron peak is sensitive, *inter alia*, to the charge density on the unionized atom and to the degree of shielding of the core-hole generated by the loss of the electron.¹⁰⁰ For carbon 1s peaks, this sensitivity manifests itself as chemical shifts to higher binding energies for carbons in higher oxidation states or with electronegative substituents. Aliphatic hydrocarbons yield a characteristic peak at 284.7 eV (referenced to Au(4f_{7/2}) at 84.0 eV) with most other functional groups appearing at higher binding energies. Figure 11 (right) shows high-resolution spectra of the C(1s) region of six monolayers. The spectrum of HS(CH₂)₁₀CH₃ (Figure 11(a)) exhibits a single, sharp, symmetrical peak. The other spectra show discrete peaks at higher binding energies arising from the functionalized carbon atoms. The large high-energy peak in the carbon 1s spectrum in Figure 11(f) arises from both the nitrile and α -methylene groups.¹⁰¹ The shifts in binding energy, Δ , from the methylene peak agree with literature values.^{102,103} We have used these values as diagnostic tools on surfaces of unknown composition and for following the progress of surface reactions.¹⁰⁴ The main methylene peaks of the carboxylic acid, ester and nitrile show pronounced asymmetry on the high binding energy side. A good fit can only be obtained by addition of an extra peak at $\Delta = 0.8 - 1.1$ eV. This peak arises from the carbon α to the carbonyl or β to the nitrile group and has an area consistent with a single carbon atom.

Stability and Reactivity of Monolayers of Alkanethiols on Gold. Although a detailed quantitative analysis of stability and reactivity is beyond the scope of this paper, some understanding of the thermal stability and chemical reactivity of thiol monolayers on gold is essential in determining the range of applications in which they can be used. Monolayers of alkanethiols on gold appear to be stable indefinitely in air, or in contact with liquid water or ethanol at room temperature (we observed no change in contact angle or thickness over a period of several months). A high flux of adsorbate molecules incident on the surface is thus not required to maintain the integrity of the monolayer. Upon heating to temperatures over 70 °C the monolayers desorbed.¹⁰⁵ The rate of desorption was dependent on the temperature, ambient medium, and chain length of the adsorbate. Qualitatively, desorption was most rapid in a hydrocarbon solvent, slower in ethanol and slower still in air. Compared to other monolayer systems, thiol monolayers are thermally more stable than long-chain amines on Cr (which desorb in cold ether⁹²), or dialkylsulfides on gold (which desorb in argon at 80 °C)⁹ but significantly less stable than silane monolayers on silicon where binding to the substrate occurs, in part, through strong, covalent Si-O bonds.

We examined the effect of chain length on thermal desorption of monolayers of five methyl-terminated thiols (C₁₀, C₁₂, C₁₆, C₁₈, C₂₂) in hexadecane at 83 °C (Figure 13). We monitored the

extent of desorption by the change in ellipsometric thickness. Figure 13 shows that long-chain thiols form monolayers that are thermally more stable than those formed from short-chain thiols. The scatter in the ellipsometric data and the inherent uncertainty in the accuracy of the technique when applied to partial monolayers¹⁰⁶ preclude a rigorous determination of the kinetic order. The curves do, however, conform at least approximately to an exponential, as expected for a first-order process. Using a highly simplified model of the desorption process, we can determine the dependence of activation energy of desorption on chain length, n . If we assume a first-order desorption process, then the rate constant can be obtained from a logarithmic plot of thickness against time (Figure 13b). In Figure 13b, the corrected thickness is the difference between the ellipsometric thickness at time t and the thickness at long times. Linear fits to the data (solid lines) yield the rate constants, k_n , for desorption. Assuming further that the desorption kinetics are described by a simple Arrhenius-like relationship with a constant pre-exponential factor, a logarithmic plot of k_n against chain length should be linear with a slope $-d(E_a/kT)/dn$, where E_a is the activation energy of desorption (Figure 14). The goodness of fit is surprising (and probably fortuitous) and yields an increase in activation energy of 0.2 kcal/mol per methylene unit.¹⁰⁷ Using a "normal" pre-exponential factor¹² of 10^{13} s^{-1} we calculate an activation energy of 28 kcal/mol for desorption of docosanethiol moieties (as the disulfide or gold thiolate)

from gold into hexadecane. Dubois et al¹², using similar assumptions, obtained an activation energy of 28 kcal/mol for desorption of dimethyl disulfide from gold in UHV by temperature-programmed desorption.

In making surface measurements, and, in particular, in executing chemical reactions at the surface, the intrinsic lability of the thiol monolayers towards some reagents is a limitation. Monolayers of octadecanethiol on gold were unaffected by immersion in 1 N HCl or 1 N NaOH for one day (that is, we observed no changes in the contact angles or ellipsometric thickness), but after one month signs of deterioration were evident. The contact angle with water on the slide immersed in base dropped by 3° over this period. In acid, more extensive deterioration was apparent: the contact angle of water dropped from 112° to 104° and of hexadecane from 48° to 44°, and the surface of the gold was visibly pitted, although ethanol still did not wet the slide. Clearly, chemicals that attack either the gold film (aqua regia, mercury, I_3^-) or the chromium adhesion promoter (conc. HCl) must be avoided. We have observed that a number of other chemicals appear to attack the monolayers themselves, including halogens (I_2 , Br_2), strong oxidizing agents (peroxide, ozone), and ethereal solutions of borane and phosphorous pentachloride. We note specifically that attempts to measure contact angles with methylene iodide, purified by distillation and passage through activated alumina, tended to cause damage to the monolayer, presumably due to the presence of either I_2 or HI

from photolysis of the methylene iodide. Susceptibility of disulfide monolayers to attack by aqueous solutions of I^- has been reported previously.¹³ We have not carried out a comprehensive study of the chemical reactivity of thiol monolayers, and we suggest caution when new reactions are attempted.

Conclusions

Ellipsometry, contact angles, and X-ray photoelectron spectroscopy indicate that alkanethiols adsorb onto evaporated, polycrystalline gold substrates and form monomolecular films. TEM diffraction patterns²² demonstrate two-dimensional order in these monolayers and infrared spectra^{18,47} suggest that the thiols form densely packed, pseudo-crystalline assemblies on the surface with an all-trans arrangement of the carbon-carbon bonds. IR data also indicate that the hydrocarbon chains have a mean tilt of 20-30° from the surface normal. Our ellipsometric data on methyl-terminated thiols yields a thickness of 1.5 Å per methylene group, consistent with previous results¹⁸ but inconsistent with a model of tilted chains or chains oriented normal to the surface. The reason for the discrepancy is not clear. If the hydrocarbon chain is longer than ten carbons, the wetting properties are largely independent of chain length and are not influenced directly by the gold-sulfur interface. Contact angles provide a very sensitive probe of the outermost few angstroms of the surface. The high contact angles of water and hexadecane on methyl-terminated thiol monolayers and the low contact angles on carboxylic acid and alcohol-terminated monolayers suggest that the surface of the monolayer comprises a densely packed array of the tail groups of the thiols. The high contact angle of hexadecane on monolayers of thiols terminated by a methyl ester or methyl ether also provides strong support for a model in which the thiols are highly oriented so that only the

methyl group is directly exposed to the contacting liquid. XPS has proven to be a very useful analytical tool for studying both the composition of the monolayer and the elemental profile normal to the surface. Angle-dependent XPS provides further confirmation for binding to the gold through the sulfur, and for the location of the tail group exclusively at the surface of the monolayer.

Despite the extensive characterization that now exists for monolayers of thiols on gold, the exact nature of the interaction between the sulfur head group and the gold surface remains enigmatic. Under UHV conditions thiols adsorb intact on the gold surface¹² but are bound only very weakly and desorb well below room temperature. When adsorbed from solution, however, thiols form monolayers that are stable well above room temperature.¹⁰⁸ Disulfides adsorbed on gold undergo extensive S-S bond scission to yield surface thiolate species.¹² Several experiments suggest that the surface species generated by adsorption of thiols from solution is similar to that produced by adsorption of disulfides: high-resolution XPS of the sulfur 2p core level yields indistinguishable spectra for solution-adsorbed monolayers of octanethiol and dioctyl disulfide;⁸⁵ TEM studies show identical lattice structures for thiols and disulfides adsorbed on the predominant (111) face of gold;²² the activation energy for desorption of a thiol monolayer into solution is comparable to that for UHV desorption of a disulfide monolayer; the rates of displacement and desorption into solution of thiols and di-

sulfides are similar.^{84,85} All these pieces of evidence point to binding of thiols to gold through a thiolate moiety but throw no light on the mechanism for conversion of the thiol to thiolate. If a thiolate is the surface species generated by adsorption of a thiol it should in principle be possible to trace the hydrogen released during the adsorption process.¹⁰⁹ The elucidation of the adsorption mechanism remains an area of active interest in our group.

An important observation in this work is the sensitivity of the contact angle of water and hexadecane to the tail group of monolayers of thiols on gold. This sensitivity not only confirms that the tail group is the predominant, or even the sole, functional group exposed at the surface of the monolayer, but also attests to the short-range nature of the molecular interactions responsible for wetting. Previous studies on less well-ordered systems^{9,110} have shown that the contact angle with water is insensitive to the presence of polar functional groups once they are buried more than 5 Å below the surface. The high contact angles of hexadecane on monolayers of methyl ether and methyl ester terminated thiols suggest that, for purely dispersive liquids on well-ordered substrates, even a single atomic layer is sufficient to decrease greatly the strength of the interactions that determine wetting.¹¹¹ This latter conclusion is strongly supported by the results of chemisorption studies in UHV that examine the interactions of adsorbates with the tail groups of thiol and disulfide monolayers.¹¹²

We have established in this paper that high-quality monolayers of thiols on gold may be prepared with a variety of adsorbates over a wide range of concentration and in many different solvents. The nature of the adsorption process and the mechanisms for desorption and displacement of preformed monolayers were not addressed in detail but are the subject of ongoing research in our laboratory.

Experimental Section.

Materials. Ethanol (U.S. Industrials Co.) was deoxygenated with bubbling N_2 for 1 h before use, when employed as a solvent for thiols, but not purified further. Hexadecane (Aldrich, 99%) was percolated twice through activated, neutral alumina. High purity hexane, methanol, methylene chloride, THF, DMF, carbon tetrachloride, acetonitrile and cyclooctane were used without further purification. Water was deionized and distilled in a glass and Teflon apparatus.

Ethanethiol (Aldrich, 99%), 1-propanethiol (Aldrich, 99%), 1-butanethiol (Aldrich, 99+%), 1-heptanethiol (Aldrich, tech), mercaptoacetic acid (Aldrich, 95%), 6-bromohexanoic acid (Aldrich, 98%), 16-hydroxyhexadecanoic acid (Aldrich, 98%), 1-bromoundecane (Aldrich, 99%), 11-bromo-1-undecene (Pfaltz and Bauer), 1-heptadecanol (Aldrich, 98%), 1,8-dibromooctane (Aldrich, 98%), t-butyldimethylsilyl chloride (Aldrich, 97%) and diisopropyl azodicarboxylate (Aldrich, 97%) were used as received.

1-Hexanethiol (Aldrich, 96%), 1-octanethiol (Aldrich, 97%), 1-decanethiol (Aldrich, 97%), 1-dodecanethiol (Aldrich, 98%) and 1-tetradecanethiol (Pfaltz & Bauer) were chromatographed using hexane as solvent. 11-Bromo-1-undecanol (Aldrich, 98%), 11-bromoundecanoic acid (Aldrich, 99+%), 1,12-dibromododecane (Aldrich, tech), 1-bromoeicosane (Alfa, 97%) and 1-bromodocosane

(Alfa, 97%) were recrystallized from hexane. 1-Nonanethiol (Aldrich, tech) was distilled at reduced pressure and chromatographed (hexanes). 1-Hexadecanethiol (Aldrich, tech) was recrystallized from ethanol, distilled at reduced pressure, and chromatographed (hexane). 1-Octadecanethiol (Aldrich, 98%) was chromatographed (hexane) and recrystallized from ethanol. Thiolacetic acid (Aldrich, tech) was distilled. Triphenyl phosphine (Aldrich, 99%) was recrystallized from ethanol-water and dried over P_2O_5 . Imidazole (Aldrich) was recrystallized from 1:1 hexane/ethyl acetate. 1H,1H,2H,2H-tridecafluoro-1-octanethiol (Telomer B Thiol, Du Pont), 96 % pure by G.C. (balance other telomers) was a gift from Dr. Nandan Rao (Du Pont).

Details of the preparation of the following molecules may be found in supplemental material to this journal: 1-undecanethiol, 1-heptadecanethiol, 1-eicosanethiol, 1-docosanethiol, 6-mercaptohexanoic acid, 11-mercaptopundecanoic acid, 16-mercaptohexadecanoic acid, 21-mercaptoheptacosanoic acid, 18-nonadecene-1-thiol, 11-(t-butyldimethylsiloxy)-1-undecanethiol, 11-bromo-1-undecanethiol, 11-chloro-1-undecanethiol, 11-methoxy-1-undecanethiol, 12-mercapto-1-dodecyl thioacetate, methyl 11-mercaptopundecanoate, 9-mercaptononanenitrile, 11-mercapto-1-undecanol, di(11-hydroxyundecyl) disulfide, diundecyl disulfide.

Preparation and Handling of Gold Substrates. Gold substrates were prepared by thermal or electron-beam evaporation of high-purity gold (99.9 - 99.999%) onto single-crystal silicon

(111) test wafers that had been pre-coated with chromium to improve adhesion (50 Å of Cr followed by 1000 - 2000 Å of Au).¹¹³ The substrates were stored in Fluoroware wafer holders until used in experiments, generally as soon as possible after evaporation. Occasionally slides were stored for several days and were then plasma-cleaned before use (Harrick PDC-23G: 20 s O₂, 0.2 Torr, low power; 20 s H₂, 0.2 Torr, low power). The resulting surface was not rigorously clean--water contact angles of 20 - 30° were observed--but monolayers with reproducible contact angles could be formed on the slides. We were unable consistently to generate good monolayers on slides that had been cleaned by oxygen plasma alone, probably due to the formation of metastable, surface, gold oxides.¹¹⁴ Before use in experiments, the 3-in wafers were cut into conveniently sized slides (ca. 1 cm x 3 cm) with a diamond-tipped stylus, rinsed with ethanol, and blown dry with a stream of high purity argon. Adsorptions were carried out in glass weighing bottles that had been cleaned with 'piranha solution' (7:3 conc. H₂SO₄/ 30% H₂O₂) at 90 °C for one hour, and rinsed exhaustively with distilled, deionized water and absolute ethanol. Caution: 'piranha solution' reacts violently with many organic materials and should be handled with great care.

Ellipsometry. Ellipsometric measurements were made on a Rudolf Research Type 43603-200E Ellipsometer using a wavelength of 6328 Å (He-Ne laser) and an incident angle of 70°. Samples were washed with ethanol and blown dry with argon before taking

measurements. Three separate points were measured on each sample and the readings then averaged. Readings were taken on the clean gold, to establish the bare substrate optical constants, and after monolayer formation, and the thicknesses calculated using a parallel, homogeneous, three-layer model⁸ with an assumed refractive index of 1.45 for the monolayer.¹¹⁵ The computer program was written by S. Wasserman based on an algorithm by McCrackin.¹¹⁶ The thickness is only moderately sensitive to the exact value of n chosen: if a value of $n = 1.47$ is substituted in the calculation, the thicknesses are decreased by ca. 2.5%. In partial monolayers, in which loose packing or island formation may occur, the uncertainty in the model is greater. The observed scatter in the data is ± 2 Å for most thiol systems. We believe that this variation reflects the imprecision of the measurements as opposed to actual variations in the monolayer thickness.

The effect of adventitiously adsorbed materials on the ellipsometric thickness has already been discussed. We also conducted specific experiments to determine the effect of storage time of the gold on the measured thickness.

Surface contamination on gold may be divided into three categories: (1) water and other reversibly adsorbed vapors, (2) organic contaminants that are removed by the ethanol washing procedure, and (3) irreversibly adsorbed contaminants. The first category will always be present in our studies since our ellipsometer is not fitted with an environmentally controlled sample chamber. The second group of contaminants, typically several

angstroms thick, is removed immediately before taking measurements. The effect of storage on the third category is amenable to investigation.

We determined the ellipsometric constants of a batch of slides shortly after evaporation and immediately immersed some of the slides in a solution of docosanethiol in ethanol. The remaining slides were stored in polypropylene containers (Fluoroware) for periods of up to one week. At intervals, slides were removed from the containers, the ellipsometric constants remeasured, and the slides immersed in the solution of docosanethiol. As Figure 15 shows, thicknesses of 30-33 Å were calculated for the slides immersed in docosanethiol immediately and for those stored for several days if the original bare substrate readings were used. However, thicknesses of only 26-30 Å were obtained on the stored substrates if the ellipsometric readings taken immediately before immersion were used. The implication of this observation is that, on storage, the gold surfaces had attracted 1-5 Å of additional contaminants that could not be removed by ethanol rinses. The constant values of the contact angles and the ellipsometric thickness using the original bare substrate readings indicate that these contaminants were displaced by the thiol. The true thickness of adventitiously adsorbed material is even greater than indicated here, since even on day zero contamination rendered the gold slides hydrophobic.⁵⁷

Contact Angles. Contact angles were determined on a Rame-Hart Model 100 Goniometer at room temperature and 100%

relative humidity for water, and ambient humidity for all other probe liquids.¹¹⁰ Under these conditions the contact angles were stable for many minutes. Contact angles were measured by two closely related techniques. In Method A, the advancing water contact angle, $\theta^{\text{air}}(\text{H}_2\text{O})$, was obtained by forming a 1- μl drop of water (2 μl for angles over 80° to improve accuracy) at the end of a PTFE-coated, blunt-ended needle attached to a 50- μl syringe fitted with a repeater, lowering the needle until the drop touched the surface, and raising the needle. As the drop detached itself from the needle tip it advanced over the surface. In method B³⁰, liquid was added to the sessile drop until the front was seen to advance across the surface. Once observable motion had ceased the contact angle was measured without removing the needle from the drop. We refer to the value obtained this way as the maximum advancing contact angle.

Zisman Plots. Contact angles were measured by Method A, at 19 °C, under an atmosphere saturated with the probe liquid. Alkanes and other hydrocarbons were percolated through neutral, grade 1 alumina immediately prior to measurement of contact angles. The alcohols were high-purity solvents and were not purified further. Surface tensions were extracted from Jasper, J.J. J. Phys. Chem. Ref. Data 1972, 1, 841-1009. The following liquids were used (surface tension in parentheses): 2,3-dimethylpentane (20.1 mN/m), n-heptane (20.2), 2,2,4-trimethylhexane (20.6), n-octane (21.7), n-nonane (22.9), n-undecane (24.8), cyclohexane (25.4), n-dodecane (25.4), n-

tetradecane (26.6), n-hexadecane (27.6), cyclooctane (29.9), bicyclohexyl (32.8), 2-propanol (21.6), ethanol (22.5), 1-propanol (23.8), 1-butanol (25.5), 1-pentanol (25.9), 1-octanol (27.6), cyclohexanol (33.5).

Scanning Electron Microscopy. The micrograph of the evaporated gold film was obtained on a JEOL JSM-35 scanning electron microscope with an accelerating potential of 35 kV, a magnification of 60000X, a working distance of 15 mm, and a sample tilt of 30°.

Kinetics Studies. We obtained plots of the kinetics of adsorption by repeated measurements on individual slides. Slides were removed from the adsorbate solution, quickly rinsed with ethanol, blown dry with a stream of argon, and the contact angles and ellipsometric constants measured before rinsing the slides once more and reimmersing them in the adsorbate solutions. The slides were also rinsed between the two sets of measurements to minimize contamination. The values of the contact angles and the ellipsometric thickness were not sensitive to the order in which they were measured. We prepared the adsorbate solutions at a concentration of 1 mM except in two experiments: in the experiment in Figure 9 the solutions were prepared by serial dilution of a 1 mM solution; in Figure 5 we prepared the adsorption solutions from stock solutions that were 4 mM in thiol or 2 mM in disulfide.

X-ray Photoelectron Spectroscopy (XPS). We obtained X-ray photoelectron spectra on an SSX-100 spectrometer (Surface Science

Instruments) equipped with an aluminum source, quartz monochromator, concentric hemispherical analyzer operating in fixed analyzer transmission mode, and multichannel detector. The pressure in the chamber during analysis was approximately 1×10^{-9} Torr. The analyzer lens had an acceptance angle of 30° . The spectra were referenced to $\text{Au}(4f_{7/2})$ at 84.00 eV, and a separation between the $\text{Cu}(2p_{3/2})$ and $\text{Cu}(3s)$ of 810.08 eV. Except where otherwise stated a take-off angle of 35° from the surface was employed. Survey spectra were recorded using a 150-eV pass energy, 1 mm spot, and 200 W electron beam power with an acquisition time of 7 minutes. We performed control experiments on representative monolayers to determine rates of beam-induced damage. The acquisition times used were sufficiently short that sample damage did not affect the spectra significantly. Specific details of these studies will be published separately.

Abundances of the minor elements (O, N, S, Br) obtained from the survey spectra were generally within 1-2 atom percent of values obtained from high resolution spectra and have been rounded to the nearest percent. Atomic compositions were derived from peak areas using photoionization cross-sections calculated by Scofield¹¹⁷, corrected for the dependence of the escape depth on the kinetic energy of the electrons (assumed to have the form $\lambda = kE^{0.7}$). With a pass energy of 150 eV, the analyzer transmission function is approximately constant over the range of binding energies studied. High resolution spectra of the $\text{C}(1s)$ region were recorded with a 50-eV pass energy, 300- μm spot and 50-W

electron beam power. The acquisition time was approximately 30 min. All the carbon spectra were fitted using symmetrical 90% Gaussian/10% Lorentzian profiles and the minimum number of peaks consistent with a reasonable fit and the molecular structure of the adsorbates. The peak shape was chosen to optimize the fit to the low binding energy side of the main methylene peak. With the exception of the peak shape, the fits were unconstrained. The spectra within each figure (Figures 11 and 12) were scaled to the same maximum peak height.

Thermal Desorption Experiments. We carried out desorptions in an unstirred glass weighing bottle partially immersed in an oil bath thermostatted at 86 ± 1 °C. The temperature of the hexadecane in the glass bottle was 83 °C. Slides (1 cm x 3 cm) with preformed monolayers were immersed in 20 mL of hot hexadecane, removed at suitable time intervals, rinsed with ethanol, blown dry with a stream of argon, and the ellipsometric constants measured. The thickness of the adsorbed organic layer was calculated using the optical constants for clean gold. Corrected thicknesses were calculated by subtracting from the ellipsometric thickness the mean of several readings obtained at long times when desorption was essentially complete. The rate constants were determined from the logarithmic plot by least-mean-square fits to data with corrected thicknesses greater than 3 Å: the error in data representing smaller thicknesses becomes very large.

Acknowledgements. XPS spectra were obtained using instrumental facilities purchased under the DARPA/URI program and maintained by the Harvard University Materials Research Laboratory NMR spectra were obtained in the Bruker NMR Facility at Harvard. We are very grateful to Dr. D. Allara, Dr. L. Strong, Dr. M. Chaudhury, and Dr. S. Wasserman for valuable discussions and to Dr. N. Rao (E.I. DuPont de Nemours) for the gift of fluorinated thiols.

REFERENCES AND NOTES

1. This research was supported in part by the Office of Naval Research and the Defence Advanced Research Projects Agency, and by the National Science Foundation (Grant CHE 85-08702).
2. IBM Pre-doctoral Fellow in Physical Chemistry 1985-86.
3. Langmuir, I. J. Am. Chem. Soc. 1917, 39, 1848-1906; Blodgett, K.B. J. Am. Chem. Soc. 1935, 57, 1007-22; Gaines, G.L. Insoluble Monolayers at Liquid-Gas Interfaces; Interscience: New York, 1966.
4. Blinov, L.M. Russian Chem. Rev. 1983, 52, 713-35; Roberts, G.G. Adv. Phys. 1985, 34, 475-512; Proceedings of The Second International Conference on Langmuir-Blodgett Films. Thin Solid Films, 1985, Volumes 132, 133, 134.
5. Bigelow, W.C.; Pickett, D.L.; Zisman, W.A. J. Colloid Sci. 1946, 1, 513-538.
6. Zisman, W.A. Adv. Chem. Ser. No.43 1964, 1-51.
7. (a) Haller, I. J. Am. Chem. Soc. 1978, 100, 8050-55; (b) Sagiv, J. J. Am. Chem. Soc. 1980, 102, 92-98; (c) Maoz, R.; Sagiv, J. J. Colloid Interface Sci. 1984, 100, 465-96 and references therein.
8. Allara, D.L.; Nuzzo, R.G. Langmuir, 1985, 1, 45-52; *ibid.* 52-66, and references cited therein.

9. Troughton, E.B.; Bain, C. D.; Whitesides, G.M.; Nuzzo, R.G.; Allara, D.L.; Porter, M.D. Langmuir 1988, 4, 365-385.
10. Woods, R. in Flotation; Fuerstenau, M. C , Ed.; American Institute of Mining, Metallurgical, and Petroleum Engineers: Baltimore, 1976.
11. Nuzzo, R.G.; Allara, D.L. J. Am. Chem. Soc. 1983, 105, 4481-83.
12. Nuzzo, R.G.; Zegarski, B.R.; Dubois, L.H. J. Am. Chem. Soc. 1987, 109, 733-40.
13. Nuzzo, R.G.; Fusco, F.A.; Allara, D.L. J. Am. Chem. Soc. 1987, 109, 2358-2368.
14. diGleria, K.; Hill, H.A.O.; Page, D.J.; Tew, D.G. J. Chem. Soc. Chem. Comm. 1986, 460-462; Taniguchi, I.; Toyosawa, K.; Yamaguchi, H.; Yasukouchi, K. J. Chem. Soc. Chem. Comm. 1982, 1032-1033; Sabatani, E.; Rubenstein, I.; Maoz, R.; Sagiv, J. J. Electroanal. Chem. 1987, 219, 365-371; Finklea, H.O.; Robinson, L.R.; Blackburn, A.; Richter, B.; Allara, D.L.; Bright, T.B. Langmuir 1986, 2, 239-244. Harris, A. L.; Chidsey, C. E. D.; Levinos, N. J.; Loiacono, D. N. Chem Phys. Lett. 1987, 141, 350-356.
15. Li, T.T.-T.; Liu, H.Y.; Weaver, M.J. J. Am. Chem. Soc. 1984, 106, 1233-39; Li, T.T.-T.; Weaver, M.J. J. Am. Chem. Soc. 1984, 106, 6107-08; Finklea, H. O.; Avery, S.; Lynch, M.; Furtsch, T.

Langmuir 1987, 3, 409-413.

16. Sundgren, J.-E.; Bodö, P.; Ivarsson, B.; Lundström, I. J. Colloid Interface Sci. 1986, 113, 530-43; Liedberg, B.; Ivarsson, B.; Lundström, I.; Salaneck, W.R. Prog. Colloid. Poly. Sci., 1985, 70, 67.75.

17. Diem, T.; Czajka, B.; Weber, B.; Regen, S.L. J. Am. Chem. Soc. 1986, 108, 6094-95.

18. Porter, M.D.; Bright, T.B.; Allara, D.L.; Chidsey, C.E.D. J. Am. Chem. Soc. 1987, 109, 3559-3568.

19. Somorjai, G.A. Chemistry in Two Dimensions - Surfaces; Cornell University Press: Ithaca, NY, 1982.

20. Bain, C. D.; Whitesides, G. M. J. Am. Chem. Soc. in press; Bain, C. D.; Evall, J.; Whitesides, G.M. unpublished results.

21. Some other functional groups, including phosphines and isonitriles, also coordinate strongly to gold.

22. Strong, L.; Whitesides, G.M. Langmuir 1988, 4, 546-558.

23. If an α,ω -dithiol is employed, loops appear to form. For example, $\text{HS}(\text{CH}_2)_{12}\text{SH}$ yielded a monolayer of thickness 10 Å and advancing contact angles $\theta^{\text{air}}(\text{H}_2\text{O})=77^\circ$ and $\theta^{\text{air}}(\text{HD})=0^\circ$.

24. Hexadecane and bicyclohexyl have low volatility and the presence or absence of saturated vapor above the sample did not affect the contact angle. With these liquids we frequently made

measurements under ambient conditions.

25. Adamson, A.W. Physical Chemistry of Surfaces; Wiley: New York, 1982; 4th ed., p 339.
26. Adamson, A.W.; Ling, I. Adv. Chem. Ser. No. 43, 1964, 57-73.
27. Young, T. Phil. Trans. Roy. Soc. (London) 1805, 95, 65-87.
28. Holmes-Farley, S.R. PhD. Thesis, Harvard, 1986.
29. Penn, L.S.; Miller, B. J. Colloid Interface Sci. 1980, 78, 238-41.
30. Dettre, R.H.; Johnson, R.E. J. Phys. Chem. 1965, 69, 1507-15.
31. Neumann, A.W.; Good, R.J. J. Colloid Interface Sci. 1972, 38, 341-58.
32. Schwartz, L.W.; Garoff, S. Langmuir 1985, 1, 219-230.
33. Schwartz, L.W.; Garoff, S. J. Colloid Interface Sci. 1985, 106, 422-37.
34. Dettre, R.H.; Johnson, R.E. Adv. Chem. Ser. No. 43 1964, 136-44.
35. Joanny, J.F.; de Gennes, P.G. J. Chem. Phys. 1984, 81, 552-62.
36. de Gennes, P.G. Rev. Mod. Phys. 1985, 57, 827-63.

37. Ray, B.R.; Bartell, F.E. J. Colloid Sci. 1953, 8, 214-23.

38. It may be argued that this technique yields the true Young contact angle on an ideal surface. On an ideal surface, however, any technique should yield the same contact angle, and on a non-ideal surface the maximum advancing contact angle may be very much greater than the Young angle -- a drop of water on a feather providing an extreme example (see also Cain, J.B.; Francis, D.W.; Venter R.D.; Neumann, A.W. J. Colloid Interface Sci. 1983, 94, 123-30; Spelt, J.K.; Absolom, D.R.; Neumann, A.W. Langmuir 1986, 2, 620-5).

39. Johnson, R.E.; Dettre, R.H. Adv. Chem. Ser. No. 43 1964, 112-35.

40. Johnson, R.E.; Dettre, R.H. J. Phys. Chem. 1964, 68, 1744-50.

41. Wenzel, R.N. Ind. Eng. Chem. 1936, 28, 988-94. This analysis does not take into account the energy of distortion of the edge of the drop.

42. The roughness factor is the ratio of the true surface area to the geometrical surface area.

43. Bartell, F.E.; Shepard, J.W. J. Phys. Chem. 1953, 57, 211-15; ibid. 455-58.

44. Shepard, J.W.; Bartell, F.E. J. Phys. Chem. 1953, 57, 458-63.

45. Abrahamsson, S.; Larsson, G.; Von Sydow, E. Acta Crystallographica 1960, 13, 770. C-C = 1.545 Å, \angle CCC = 110.5°.
46. Handbook of Chemistry and Physics; Weast, R. C., Ed.; CRC: Boca Raton, FL, 1984. C-S = 1.81 Å, C-H = 1.1 Å, C-O (in RCO₂H) = 1.36 Å. Contribution from S⁻ estimated at 1.5 Å.
47. Nuzzo, R.G.; Dubois, L.H.; Allara, D.L. unpublished results.
48. Andrade, J.D. In Surface and Interfacial Aspects of Biomedical Polymers; Andrade, J. D., Ed.; Plenum: New York, 1985; Volume 1 p255.
49. Canning, N.D.S.; Outka, D.; Madix, R.J. Surf. Sci. 1984, 141, 240-254.
50. Chesters, M.A.; Somorjai, G.A. Surf. Sci. 1975, 52, 21-28.
51. Trapnell, B.M.W. Proc. Roy. Soc. London Ser. A 1953, A218, 566-77.
52. Richer, J.; Stolberg, L.; Lipkowski, J. Langmuir 1986, 2, 630-38; Krim, J. Thin Solid Films 1986, 137, 297-303.
53. Boyd, G.E.; Livingston, H.K. J. Am. Chem. Soc. 1942, 64, 2383-88.
54. Harkins, W.D.; Loeser, E.H. J. Chem. Phys. 1950, 18, 556-60.
55. Loeser, E.H.; Harkins, W.D.; Twiss, S.B. J. Phys. Chem. 1953, 57, 251-54.

56. Busscher, H.J.; Kip, G.A.M.; Van Silfhout, A.; Arends, J. Colloid Interface Sci. 1986, 114, 307-13.
57. Gaines, G.L. Jr. J. Colloid Interface Sci. 1981, 79, 295.
58. Schneegans, M.; Menzel, E. J. Colloid Interface Sci. 1982, 88, 97-99.
59. Smith, T, J. Colloid Interface Sci. 1980, 75, 51-55.
60. We estimated this thickness by the comparing the ratio of the abundances of carbon + oxygen to gold on "clean" gold, to those on gold coated with monolayers of methyl-terminated thiols.
61. Hu, P.; Adamson, A.W. J. Colloid Interface Sci. 1977, 59, 605-14. Tadros, M.E.; Hu, P.; Adamson, A.W. J. Colloid Interface Sci. 1974, 49, 184-95.
62. Bewig, K.; Zisman, W.A. Adv. Chem. Ser. No.33, 1961, 100.
63. Graham, D. J. Phys. Chem. 1962, 66, 1815-18.
64. Vogel, V.; Woell, C. J. Chem. Phys. 1986, 84, 5200-04.
Garoff, S.; Hall, R. B.; Deckman, H. W.; Alvarez, M. S. Proc. Electrochem. Soc. 1985, 112, 85-88.
65. XPS of the carbon 1s region of a monolayer of $\text{HS}(\text{CH}_2)_2(\text{CF}_2)_5\text{CF}_3$ on gold shows no detectable adventitious carbon ($< 1 \text{ \AA}$) under UHV.
66. Bain, C.D.; Whitesides, G. M. submitted to J. Phys. Chem.

67. Fenstermaker, C. A.; McCrackin, F. L. Surf. Sci., 1969, 16, 85-96. A referee has suggested that the effect of roughness would be to compound the inconsistency between the observed and predicted slopes in the ellipsometric data.

68. The liquid may interact with the gold either by penetration through a thin monolayer or by long-range interactions. Preliminary calculations (M. Chaudhury, unpublished results) indicate that long-range dispersion interactions between a contacting liquid and gold plasmons or dipolar interactions with an array of Au-S dipoles at the gold-monolayer interface are too small to account for the observed decrease in contact angles for short chains.

69. Holmes-Farley, S. R.; Bain, C. D.; Whitesides, G. M. Langmuir, in press.

70. For comparative studies on polymer surfaces, see Scarmoutzos, L. M.; Whitesides, G.M. manuscript in preparation. Strong IR peaks from adsorbed water have also been observed in similar systems (Allara, D. L. unpublished results).

71. Bain, C. D.; Whitesides, G. M. Science 1988, 240, 62-63.

Bain, C. D.; Whitesides, G. M. J. Am. Chem. Soc. 1988, 110, 3665-3666.

72. Adam, N.K. Adv. Chem. Ser. No. 43 1964, 52-56.

73. Hare, E.F.; Shafrin, E.G.; Zisman, W.A. J. Phys. Chem. 1954, 58, 236-9.

74. We are unable to rationalize the observed contact angles using Neumann's equation of state theory (Neumann, A. W.; Good, R. J.; Hope, C. J.; Sejpal, M. J. Colloid Interface Sci. 1974, 49, 291-304).

75. Shafrin, E.G.; Zisman, W.A. J. Phys. Chem. 1962, 66, 740-48.

76. The contact angles were not time-dependent, nor was the contact angle of hexadecane affected by prior washing with water. Any reconstruction must be fast and reversible. See also Holmes-Farley, S. R.; Reamey, R. H.; Nuzzo, R. G.; McCarthy, T. J.; Whitesides, G. M. Langmuir, 1987, 3, 799-815.

77. Price, A.H. In Dielectric Properties and Molecular Behaviour; Van Nostrand Reinhold: London, 1969.

78. Eick, J.D.; Good, R.J.; Neumann, A.W. J. Colloid Interface Sci. 1975, 53, 235-48.

79. Fox, H.W.; Zisman, W.A. J. Colloid Sci. 1954, 5, 514-31.

80. The critical surface tension, γ_c , is equal to the surface tension of a liquid which just wets a solid surface and may be identified with the solid-vapor interfacial tension γ_{sv} . The critical surface tension is generally obtained by a linear extrapolation of a straight line through data from a homologous series of liquids, since roughness and contamination effects are greatest at low θ . The critical surface tension is useful in attempting comparisons between different substrates or in drawing

correlations between wetting and constitution. It has the distinct advantage that it should be largely independent of the means by which the advancing angle is measured, though it will still be influenced by the roughness of the surface. (According to Wenzel's relation,⁴¹ roughness should increase γ_C .) Many of the ambiguities involved in comparing contact angles of water on various surfaces are avoided by comparing γ_C .

81. Fowkes, F.M. Ind. Eng. Chem. 1964, 56(12), 40-52.

82. The effect of the nature of the liquid on the contact angle was more marked for the methyl ester surface of $\text{HS}(\text{CH}_2)_{10}\text{CO}_2\text{CH}_3$ adsorbed on gold. Polar liquids, which can interact by dipole-dipole or hydrogen bonding interactions, yielded lower angles than purely dispersive liquids. For example, hexadecane ($\gamma_{LV} = 27.5 \text{ mN/m}$) exhibited an advancing contact angle of 28° but the surface was wet by acetonitrile ($\gamma_{LV} = 29.3 \text{ mN/m}$).

83. The values of γ_C on the fluorinated surfaces were determined with hydrocarbon liquids. The geometric mean approximation appears to break down for fluorocarbon-hydrocarbon interfaces and thus these values may not be directly comparable with values of γ_C determined from hydrocarbon-hydrocarbon interfaces. For example, perfluorodecalin ($\gamma_{LV} = 18.3 \text{ mN/m}$) exhibits an advancing contact angle of 35° on a monolayer of octadecanethiol ($\gamma_C = 19.3 \text{ mN/m}$, calculated from contact angles of hydrocarbons).

84. Monolayers formed from undecanethiol and diundecyl disulfide were immersed in solutions of 11-hydroxyundecanethiol and di-(11-hydroxyundecyl) disulfide. The extent of displacement of the initial monolayer was monitored by the contact angle with water. 11-hydroxyundecanethiol displaced both monolayers at comparable rates. These rates were significantly faster than for displacement of the monolayers by di-(11-hydroxyundecyl) disulfide.

85. Bain, C.D. unpublished results

86. Recent electron diffraction results²² indicate that, on the predominant (111) face of gold, thiols and disulfides adsorb to give indistinguishable species. On the (100) face, however, two additional phases were observed for disulfides which were not evident in the monolayers of alkyl thiols in the study.

87. Gun, J.; Sagiv, J. J. Colloid Interface Sci. 1986, 112, 457-72.

88. A slide is autophobic if the solvent peels back to leave a dry surface when the slide is removed from the solvent.

89. Levine, O.; Zisman, W.A. J. Phys. Chem. 1957, 61, 1188-96; Bewig, K.W.; Zisman, W.A. J. Phys. Chem. 1963, 67, 130-35.

90. Bartell, L.S.; Betts, J.F. J. Phys. Chem. 1960, 64, 1075-76.

91. Cook, H.D.; Ries, H.E. J. Phys. Chem. 1959, 63, 226-230.

92. Bartell, L.S.; Ruch, R.J. J. Phys. Chem. 1956, 60, 1231-34;
ibid. 1959, 63, 1045-49.
93. Shafrin, E.G.; Zisman, W.A. J. Phys. Chem. 1957, 61, 1046-53.
94. Although the thickness of the sample placed in the 0.1 mM solution of octadecanethiol never attained the customary limiting value, the contact angles were consistent with the formation of a good monolayer.
95. Troughton, E.B. unpublished results
96. Briggs, D.; Seah, M. P. Practical Surface Analysis; Wiley: Chichester, England, 1983.
97. Fadley, C. S.; Baird, R. J.; Siekhaus, W. J.; Novakov, T.; Bergstrom, S. A. L. J. Electron. Spectrosc. 1974, 4, 93-137.
98. More precise atomic compositions can be obtained from high resolution spectra of the individual core levels but these compositions must be corrected for variations in the analyser lens transmission function, are no more accurate and yield little additional information.
99. Bussing, T. D.; Holloway, P. H. J. Vac. Sci. Tech. A 1985, 3, 1973-1981.
100. Egelhoff, W.F. Surf. Sci. Rep. 1987, 6, 253-415.
101. Ref. 96, p 363.

102. Gelius, U.; Heden, P.F.; Lindberg, B.J.; Manne, R.; Nordberg, R.; Nordling, C.; Siegbahn, K. Physica Scripta 1970, 2, 70-80.

103. Clark, D. T.; Thomas, H. R. J. Poly. Sci. Poly. Chem. Ed. 1976, 14, 1671-1700.

104. Scarmoutzos, L. M.; Bain, C. D. unpublished results.

105. Various means exist of increasing the thermal stability of monolayers, including the use of a more strongly-bound head group, increasing intra-chain interactions, and cross-linking of the adsorbate molecules by polymerization of the monolayer. These are areas of continuing research in our group.

106. There is no a priori reason why the ellipsometric readings should be linear functions of the amount of adsorbed material in partial monolayers, since the optical constants may vary with coverage, but in radiotracer experiments with octadecylamine monolayers on chromium such a linear relationship was observed.⁸⁷

107. This value of 0.2 kcal/mol of CH₂ groups (0.1 kcal/mol of CH₂ groups if the monolayer components desorb as disulfides, each molecule of which contains two polymethylene chains) is much smaller than the intra-chain van der Waals interaction energy (1.8 kcal/mol of CH₂ groups (Salem, L. J. Chem. Phys., 1962, 37, 2100-2113)) or the heat of fusion of long-chain paraffins (0.6 kcal/mol of CH₂ groups). Our assumption of zero activation entropy of desorption, S_a , is certainly incorrect in detail, and

may mask a systematic increase in S_a with chain length that compensates for changes in the activation enthalpy. If we assume that the change in the activation enthalpy is given by the value of the heat of fusion, $\Delta E_a = 0.6$ kcal/mol of CH_2 groups (which is plausible for desorption into hexadecane), then $\Delta S_a \sim +1$ cal/K per mole of CH_2 groups. This value is comparable to the change in entropy of fusion with chain length. The increased thermal stability of long-chain thiols is mirrored by preferential adsorption of longer chains in competitive adsorption experiments.⁷¹

108. The most probable explanation for the difference between UHV and solution behaviour is that the activation barrier to chemisorption is greater than the barrier to desorption of the thiol from its physisorbed state.

109. Adsorption of thiols from solution does not appear to require the presence of an oxidizing agent (Biebuyck, H. unpublished results) and surface hydrides are not stable on gold above 200 K (Lisowski, E.; Stobinski, L.; Dus, R. Surf. Sci. 1987, 188, L735-741 and references therein). Thus, molecular hydrogen appears to be the most probable final product.

110. (a) Holmes-Farley, S.R.; Reamey, R.H.; McCarthy, T.J.; Deutch, J.; Whitesides, G.M. Langmuir 1985, 1, 725-40; (b) Holmes-Farley, S.R.; Whitesides, G.M. Langmuir 1986, 2, 266-81; (c) Holmes-Farley, S.R.; Whitesides, G.M. Langmuir 1987, 3, 62-75.

111. Bain, C. D.; Whitesides, G. J. J. Am. Chem. Soc. in press.
112. (a) Dubois, L.H.; Zegarski, B. R.; Nuzzo, R. G. unpublished results; (b) Dubois, L. H.; Zegarski, B. R.; Nuzzo, R. G. Proc. Nat. Acad. Sci. 1987, 84, 4739-4742.
113. Full details on the preparation and characterization of gold substrates suitable for use in monolayer adsorption experiments will be published elsewhere.
114. After treatment with an oxygen plasma an additional Au(4f_{7/2}) peak appears in the XPS spectrum at 85.7 eV. This peak disappears upon exposure to a hydrogen plasma.
115. This refractive index was chosen by consideration of the refractive indices of hydrocarbons (hexadecanethiol (liquid) = 1.435, octacosane (solid) = 1.452) and mercaptans (decanethiol (liquid) = 1.457, octadecanethiol (solid) = 1.464 (Handbook of Chemistry and Physics; Weast, R. C., Ed.; CRC: Boca Raton, FL, 1984.))
116. McCrackin, F.L.; Passaglia, E.; Stromberg, R.R.; Steinberg, H.L. J. Res. Natl. Bur. Stand., Sect. A 1963, 67, 363-377.
117. Scofield, J. H. J. Electron Spectrosc. 1976, 8, 129.
118. Adam, N.K.; Elliott, G.E.P. J. Chem. Soc. 1962, 2206-09.
119. Fox, H.W.; Zisman, W.A. J. Colloid Sci. 1952, 7, 428-42.
120. Spelt, J. K.; Neumann, A. W. Langmuir 1987, 3, 588-91.

121. Cohen, S.R.; Naaman, R.; Sagiv, J. J. Phys. Chem. 1986, 90, 3054-56.
122. Tillman, N.; Ulman, A.; Schildkraut, J. S.; Penner, T. C. J. Am. Chem. Soc. in press.
123. Shafrin, E.G.; Zisman, W.A. J. Colloid Sci. 1952, 7, 166-77.
124. Ellison, A.H.; Zisman, W.A. J. Phys. Chem. 1954, 58, 260-65

FIGURE CAPTIONS

Figure 1. Monolayers of n-alkanethiols, $\text{CH}_3(\text{CH}_2)_n\text{SH}$, on gold. (a) Ellipsometric thickness. The dotted (dashed) line represents the thickness expected theoretically for a close-packed monolayer oriented normal (tilted 30° from the normal) to the surface. (b) Advancing contact angles: (●) hexadecane, (○) water, Method A, (□) water, Method B.

Figure 2. Monolayers of ω -mercapto-carboxylic acids, $\text{HS}(\text{CH}_2)_n\text{CO}_2\text{H}$, on gold (a) Ellipsometric thickness. The dotted (dashed) line represents the thickness expected theoretically for a close-packed monolayer oriented normal (tilted 30° from the normal) to the surface. (b) Advancing contact angles of water.

Figure 3. Scanning Electron Micrograph of a thermally evaporated gold film. A 1000 Å bar is shown.

Figure 4. Zisman plot for a monolayer of $\text{CH}_3(\text{CH}_2)_{21}\text{SH}$ on gold: (●) n-alkanes, (■) other hydrocarbons, (◇) alcohols. Contact angles were measured by Method A. The dotted line is the extrapolation used to estimate the critical surface tension, γ_c , from the data for alkanes and other hydrocarbons.

Figure 5. Competitive adsorption of thiols and disulfides from ethanol. $\chi_{\text{RSH}} = [\text{RSH}] / ([\text{RSH}] + 2[\text{R}_2\text{S}_2])$ in solution, (●) $\text{HS}(\text{CH}_2)_{10}\text{CH}_3 + [\text{S}(\text{CH}_2)_{11}\text{OH}]_2$, (□) $\text{HS}(\text{CH}_2)_{11}\text{OH} + [\text{S}(\text{CH}_2)_{10}\text{CH}_3]_2$. (a) Ellipsometric thickness (b) advancing contact angle of water (Method A) (c) advancing contact angle of hexadecane.

Figure 6. Kinetics of adsorption of octadecanethiol (solid symbols) and decanethiol (open symbols) from ethanol onto gold. (a) Ellipsometric thickness. The error bar indicates the range of values obtained on a single gold slide. (b) Advancing contact angles (Method A): (●,○) water, (■,□) hexadecane (HD).

Figure 7. Effect of contamination on kinetics of adsorption of octadecanethiol: (●) "clean" gold, (◇) gold with a preformed monolayer of propanethiol. Thicknesses were measured by ellipsometry.

Figure 8. Kinetics of adsorption for different tail groups. (a) Ellipsometric thickness: (●) $\text{HS}(\text{CH}_2)_{15}\text{CO}_2\text{H}$, (○) $\text{HS}(\text{CH}_2)_{17}\text{CH}_3$. (b) Advancing contact angle of water on $\text{HS}(\text{CH}_2)_{15}\text{CO}_2\text{H}$ (Method A). The dotted line represents the upper limit below which we regard a surface to be wetted by water.

Figure 9. Kinetics of adsorption of octadecanethiol from ethanol as a function of concentration: (a) ellipsometric thickness (b) advancing contact angle of hexadecane (HD). EtOH (●) indicates pure ethanol containing no thiol.

Figure 10. Effect of solvent on formation of hexadecanethiol monolayers. Slides were immersed overnight in 1 mM solutions at room temperature. (a) Ellipsometric thickness. The error bar indicates the range of values found upon repeated measurement of a single gold slide. (b) Advancing contact angles (Method A): (●) water, (○) hexadecane.

Figure 11. XPS of thiol monolayers on gold: survey spectra (left) and high resolution spectra of the carbon 1s region (right). Dotted lines represent computer-generated peak fits using 90% Gaussian/10% Lorentzian peak shapes. Numbers above the peaks indicate shifts in binding energy from the principal methylene peak. (a) $\text{HS}(\text{CH}_2)_{10}\text{CH}_3$ (b) $\text{HS}(\text{CH}_2)_{10}\text{CH}_2\text{OH}$ (c) $\text{HS}(\text{CH}_2)_{10}\text{CO}_2\text{H}$ (d) $\text{HS}(\text{CH}_2)_{10}\text{CO}_2\text{CH}_3$ (e) $\text{HS}(\text{CH}_2)_{10}\text{CH}_2\text{Cl}$ (f) $\text{HS}(\text{CH}_2)_8\text{CN}$.

Figure 12. Angle-dependent XPS of the carbon 1s region of a monolayer of $\text{HS}(\text{CH}_2)_{10}\text{CO}_2\text{CH}_3$ adsorbed on gold. Take-off angles of 90° (solid line) and 15° (broken line) are shown.

Figure 13. Thermal desorption of monolayers of thiols on gold in contact with hexadecane at 83 °C. (\blacktriangle) docosanethiol, (\square) octadecanethiol, (\bullet) hexadecanethiol, (\circ) dodecanethiol, (\blacksquare) decanethiol. (a) Ellipsometric thickness; inset shows complete desorption profiles for the two longest chain thiols. (b) First-order plot of the corrected thicknesses against time. $T_t - T_\infty$ represents the difference in ellipsometric thickness between time t and long times. Solid lines are linear fits to data points with $T_t - T_\infty > 3 \text{ \AA}$.

Figure 14. Logarithmic plot of the first-order rate constants for the thermal desorption of thiols from gold in hexadecane at 83 °C. The slope yields a change in activation energy for desorption of 0.2 kcal/methylene group per mole of desorbed molecules.

Figure 15. Effect of contamination of gold on ellipsometric thickness (a) and contact angle (b). Squares and circles represent two separate experiments. The abscissa represents the time of storage between the evaporation of the gold and monolayer formation. Ellipsometric thickness was calculated using constants determined immediately prior to immersion in the adsorbate solution (\circ, \square) and using initial bare substrate readings obtained shortly after evaporation (\bullet). The solid symbols (\bullet) indicate the thickness of accumulated contaminants.

Table I. Advancing Contact Angles on Thiol Monolayers Adsorbed on Gold

RSH	$\theta_a^{a,b}$	
	H ₂ O	HD
HS(CH ₂) ₂ (CF ₂) ₅ CF ₃	118	71
HS(CH ₂) ₂₁ CH ₃	112	47
HS(CH ₂) ₁₇ CH=CH ₂	107	39
HS(CH ₂) ₁₁ OSi(CH ₃) ₂ (C(CH ₃) ₃)	104	30
HS(CH ₂) ₁₁ Br	83	0
HS(CH ₂) ₁₁ Cl	83	0
HS(CH ₂) ₁₁ OCH ₃	74	35
HS(CH ₂) ₁₂ SCOCH ₃	70	0
HS(CH ₂) ₁₀ CO ₂ CH ₃	67	28
HS(CH ₂) ₈ CN	64	0
HS(CH ₂) ₁₁ OH	0	0
HS(CH ₂) ₁₅ CO ₂ H	0	0

^a Measured by Method A. ^b "0" is used to represent drops with irregular drop shapes and contact angles < 10°.

Table II. Contact Angles on Hydrocarbon Surfaces

Material	H ₂ O			HD ^d	BCH ^e	Ref
	θ_{Max}^a	θ_{Eq}^b	θ_{Mean}^c			
Paraffin Wax	129		114			118
	112		112			37
Hexamethylethane	130		115			118
Hexatriacontane		111		46		119
		104.6 ^f		46		120
Octadecyltrichlorosilane/Si		113		46	51	121
		111		45	48	122
Arachidic acid/ZnSe		110		47	53	86
Arachidic acid/Al		109		43		8
S[(CH ₂) ₁₇ CH ₃] ₂ /Au	112					9
HS(CH ₂) ₁₇ CH ₃ /Au	115	112	111	47	55	This work
C ₁₅ , C ₁₆ , C ₁₇ cycloalkanes	110		105			118
Polyethylene		102		0		110

^a Maximum advancing contact angle. ^b Drops allowed to equilibrate before measurement. ^c Arithmetic mean of maximum advancing and minimum receding contact angle. ^d Hexadecane. ^e Bicyclohexyl. ^f Indirect measurement from capillary rise on a vertical plate.

Table III. Critical Surface Tensions γ_c

	γ_c (mN/m)	Ref
$\text{CF}_3(\text{CF}_2)_{10}\text{CO}_2\text{H}/\text{Pt}$	6	73
Teflon	18	124
$\text{CH}_3(\text{CH}_2)_{21}\text{SH}/\text{Au}$	19	this work
$\text{CH}_3(\text{CH}_2)_{17}\text{SiCl}_3/\text{Si}$	20	122
Hexatriacontane	22	119
$\text{CH}_3(\text{CH}_2)_{17}\text{NH}_2/\text{Pt}$	24	123
Polyethylene	31	124

Table IV. Atomic Concentrations (%) of Monolayers of Thiols on Gold

RSH	Expected Composition					Observed Composition ^a				
	C	S	O	N	Cl	C	S	O	N	Cl
HS(CH ₂) ₁₀ CH ₃	91.7	8.3	-	-	-	97	3	-	-	-
HS(CH ₂) ₁₀ CO ₂ H	78.6	7.1	14.3	-	-	76	5	19	-	-
HS(CH ₂) ₁₁ OH	84.6	7.7	7.7	-	-	84	4	12	-	-
HS(CH ₂) ₁₀ CO ₂ CH ₃	80.0	6.7	13.3	-	-	81	4	15	-	-
HS(CH ₂) ₁₁ Cl	84.6	7.7	-	-	7.7	86	3	-	-	11
HS(CH ₂) ₈ CN	81.8	9.1	-	9.1	-	82	5	-	13	-

^a Derived from XPS survey spectra shown in Figure 11. The peak areas were converted to percentages using Scofield cross-sections¹¹⁷ corrected for the dependence of the escape depth on kinetic energy. We made no correction for the elemental depth profile of the monolayer.

Table V. Atomic Composition of a Monolayer of $\text{HS}(\text{CH}_2)_{10}\text{CO}_2\text{CH}_3$ on Gold, Derived from Angle-dependent XPS

Element (%) or Ratio of Elements	Take-Off Angle		
	90°	35°	15°
Au	44	31	17
C	44	55	66
O	8	12	17
S	4	2	1
C/O	5.8	4.7	4.1
C/S	10	30	60

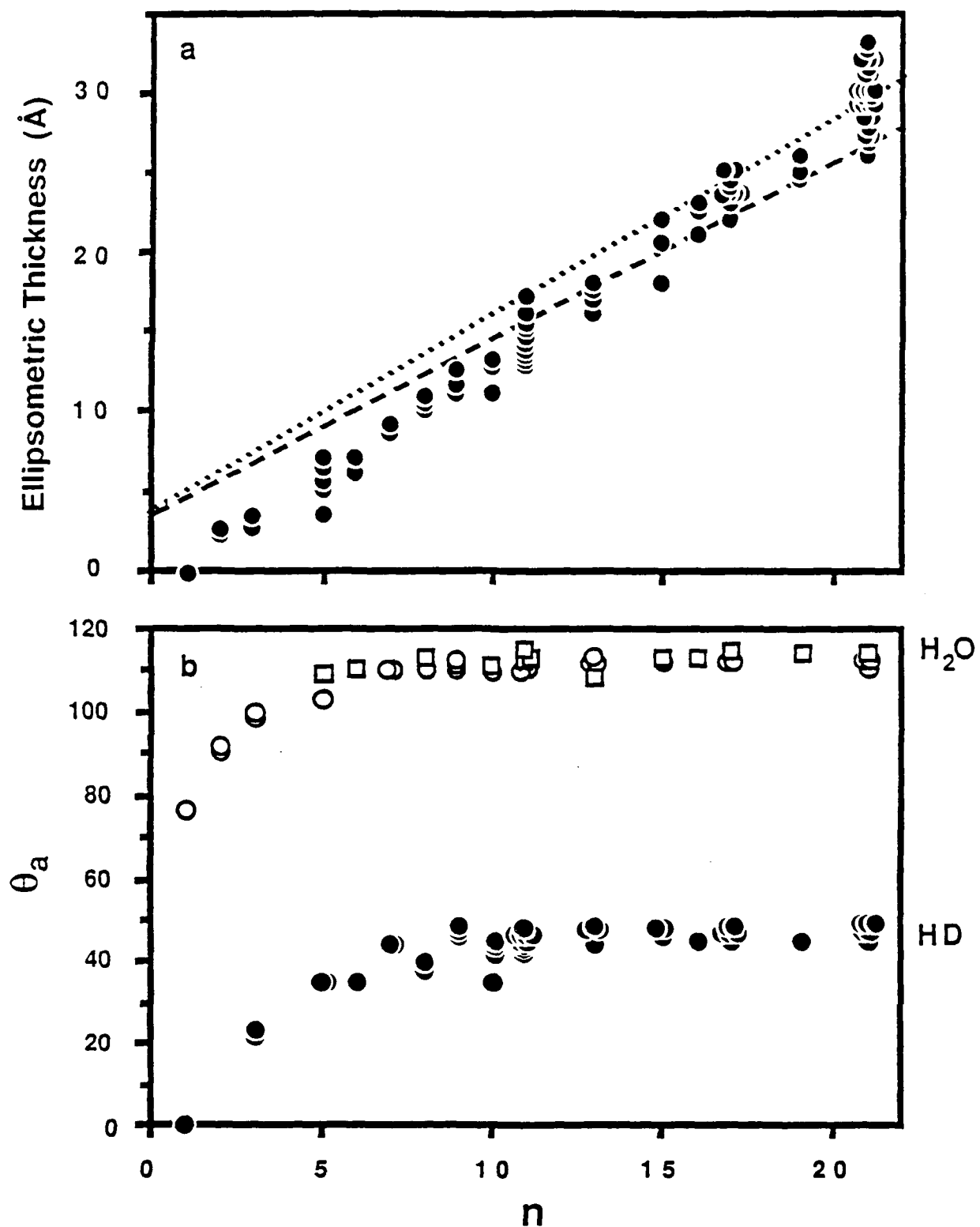


Figure 1. Monolayers of n-alkanethiols, $\text{CH}_3(\text{CH}_2)_n\text{SH}$, on gold. (a) Ellipsometric thickness. The dotted (dashed) line represents the thickness expected theoretically for a close-packed monolayer oriented normal (tilted 30° from the normal) to the surface. (b) Advancing contact angles: (\bullet) hexadecane, (\circ) water, Method A, (\square) water, Method B.

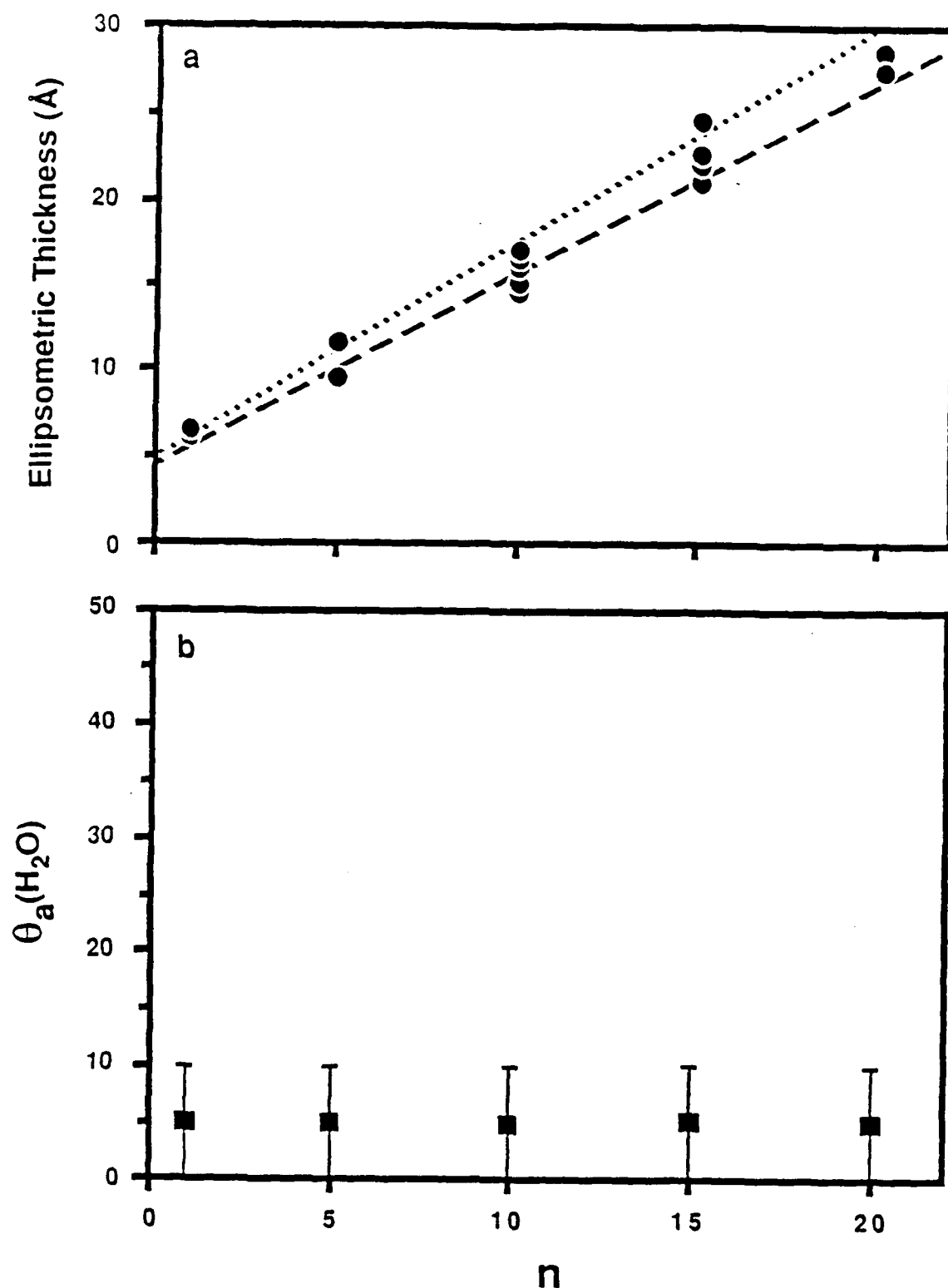


Figure 2. Monolayers of ω -mercapto-carboxylic acids, $\text{HS}(\text{CH}_2)_n\text{CO}_2\text{H}$, on gold (a) Ellipsometric thickness. The dotted (dashed) line represents the thickness expected theoretically for a close-packed monolayer oriented normal (tilted 30° from the normal) to the surface. (b) Advancing contact angles of water.

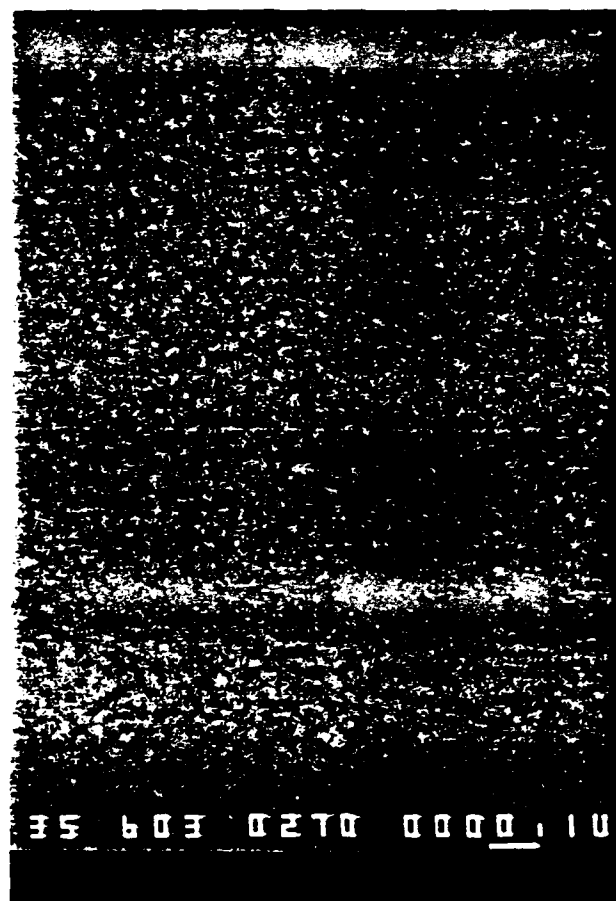


Figure 3. Scanning Electron Micrograph of a thermally evaporated gold film. A 1000 Å bar is shown.

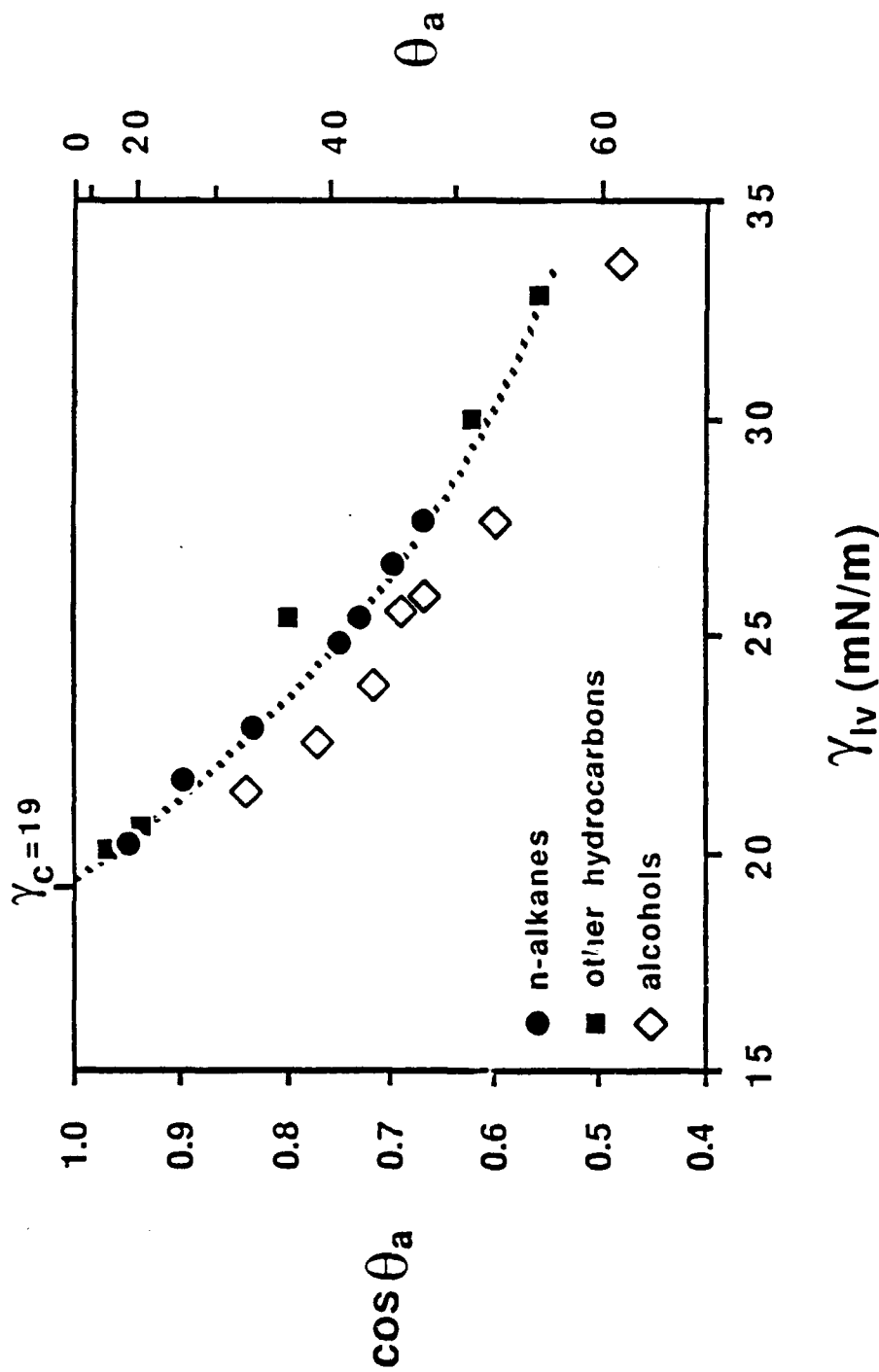


Figure 4. Zisman plot for a monolayer of $\text{CH}_3(\text{CH}_2)_{21}\text{SH}$ on gold: (●) n-alkanes, (■) other hydrocarbons, (◇) alcohols. Contact angles were measured by Method A. The dotted line is the extrapolation used to estimate the critical surface tension, γ_c , from the data for alkanes and other hydrocarbons.

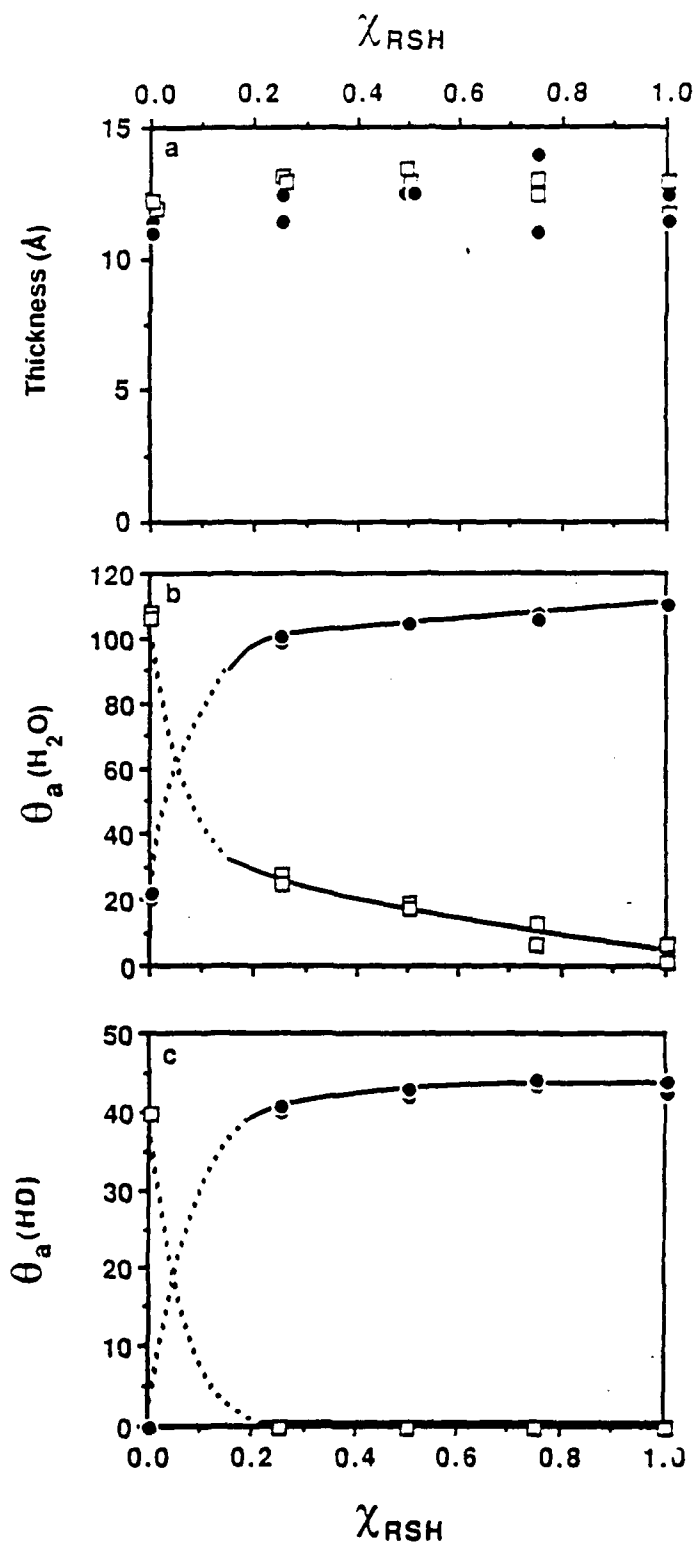


Figure 5. Competitive adsorption of thiols and disulfides from ethanol. $\chi_{RSH} = [RSH]/([RSH] + 2[R_2S_2])$ in solution, (●) $HS(CH_2)_{10}CH_3 + [S(CH_2)_{11}OH]_2$, (□) $HS(CH_2)_{11}OH + [S(CH_2)_{10}CH_3]_2$. (a) Ellipsometric thickness (b) advancing contact angle of water (Method A) (c) advancing contact angle of hexadecane.

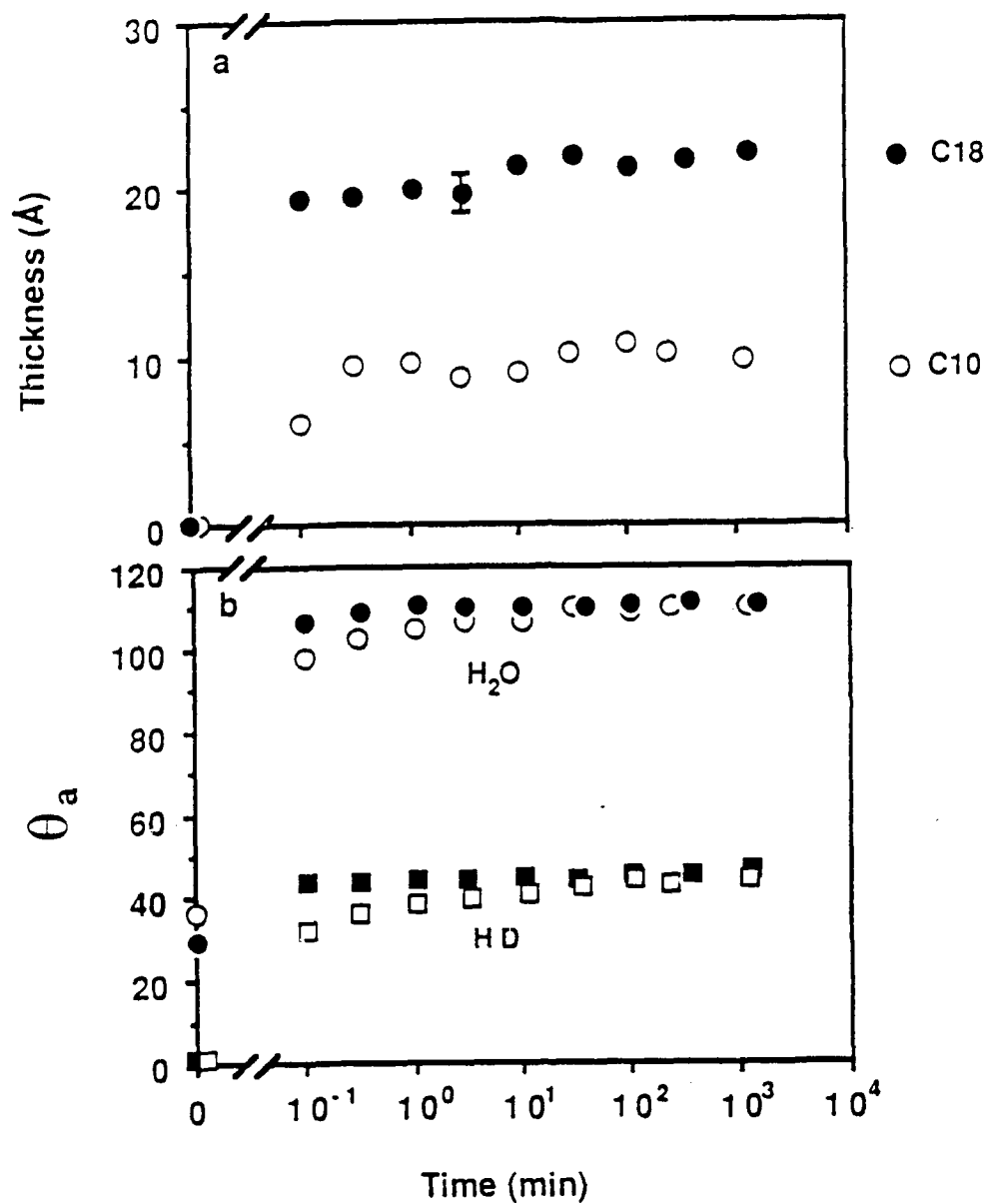


Figure 6. Kinetics of adsorption of octadecanethiol (solid symbols) and decanethiol (open symbols) from ethanol onto gold. (a) Ellipsometric thickness. The error bar indicates the range of values obtained on a single gold slide. (b) Advancing contact angles (Method A): (\bullet , \circ) water, (\blacksquare , \square) hexadecane (HD).

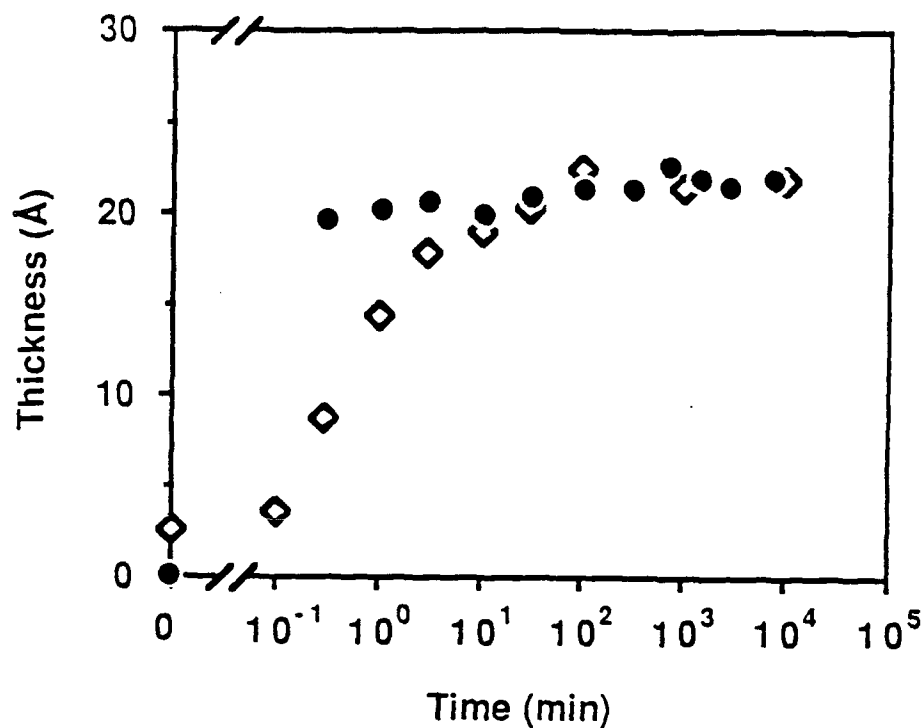


Figure 7. Effect of contamination on kinetics of adsorption of octadecanethiol: (●) "clean" gold, (◊) gold with a preformed monolayer of propanethiol. Thicknesses were measured by ellipsometry.

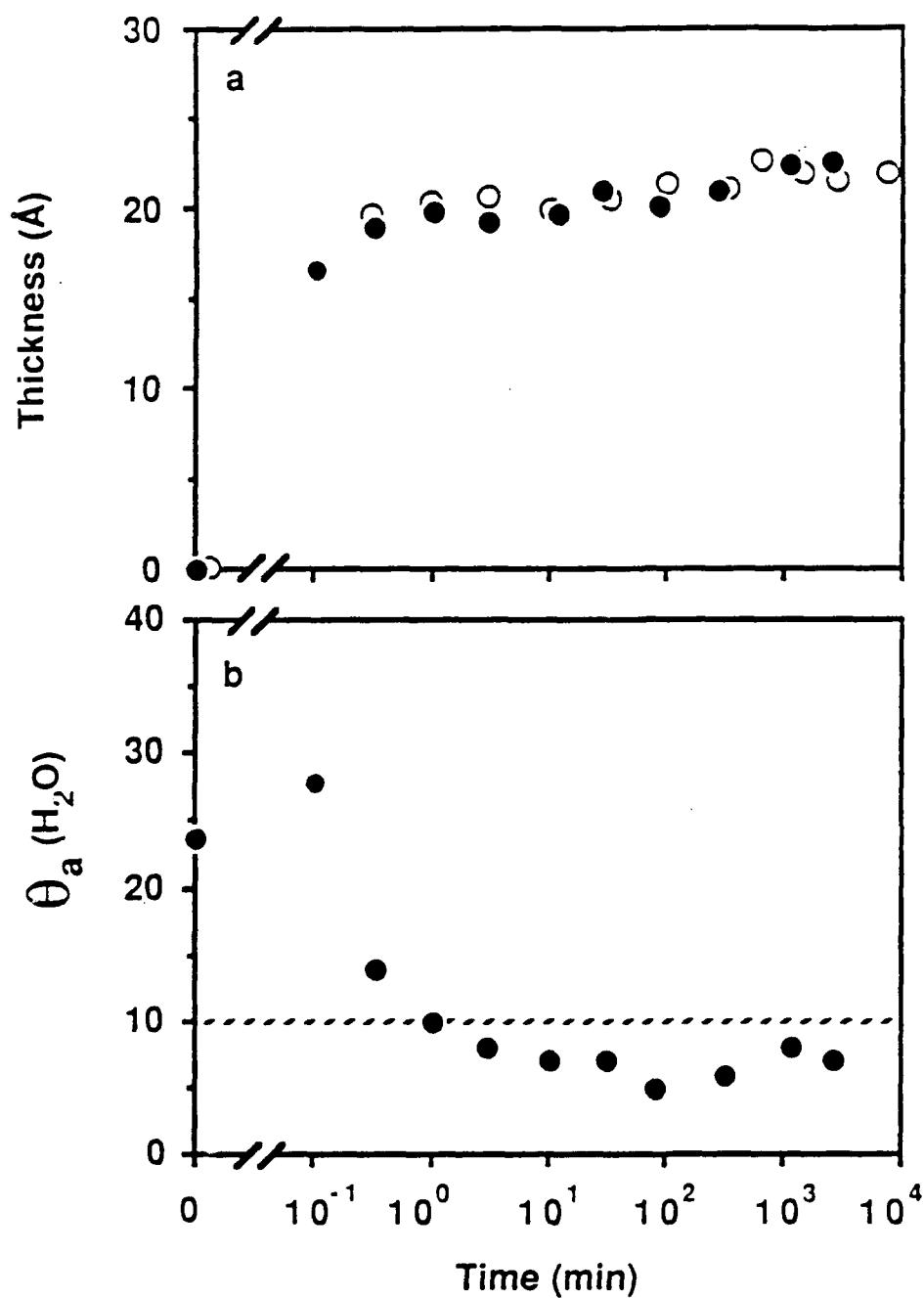


Figure 8. Kinetics of adsorption for different tail groups. (a) Ellipsometric thickness: (●) $\text{HS}(\text{CH}_2)_{15}\text{CO}_2\text{H}$, (○) $\text{HS}(\text{CH}_2)_{17}\text{CH}_3$. (b) Advancing contact angle of water on $\text{HS}(\text{CH}_2)_{15}\text{CO}_2\text{H}$ (Method A). The dotted line represents the upper limit below which we regard a surface to be wetted by water.

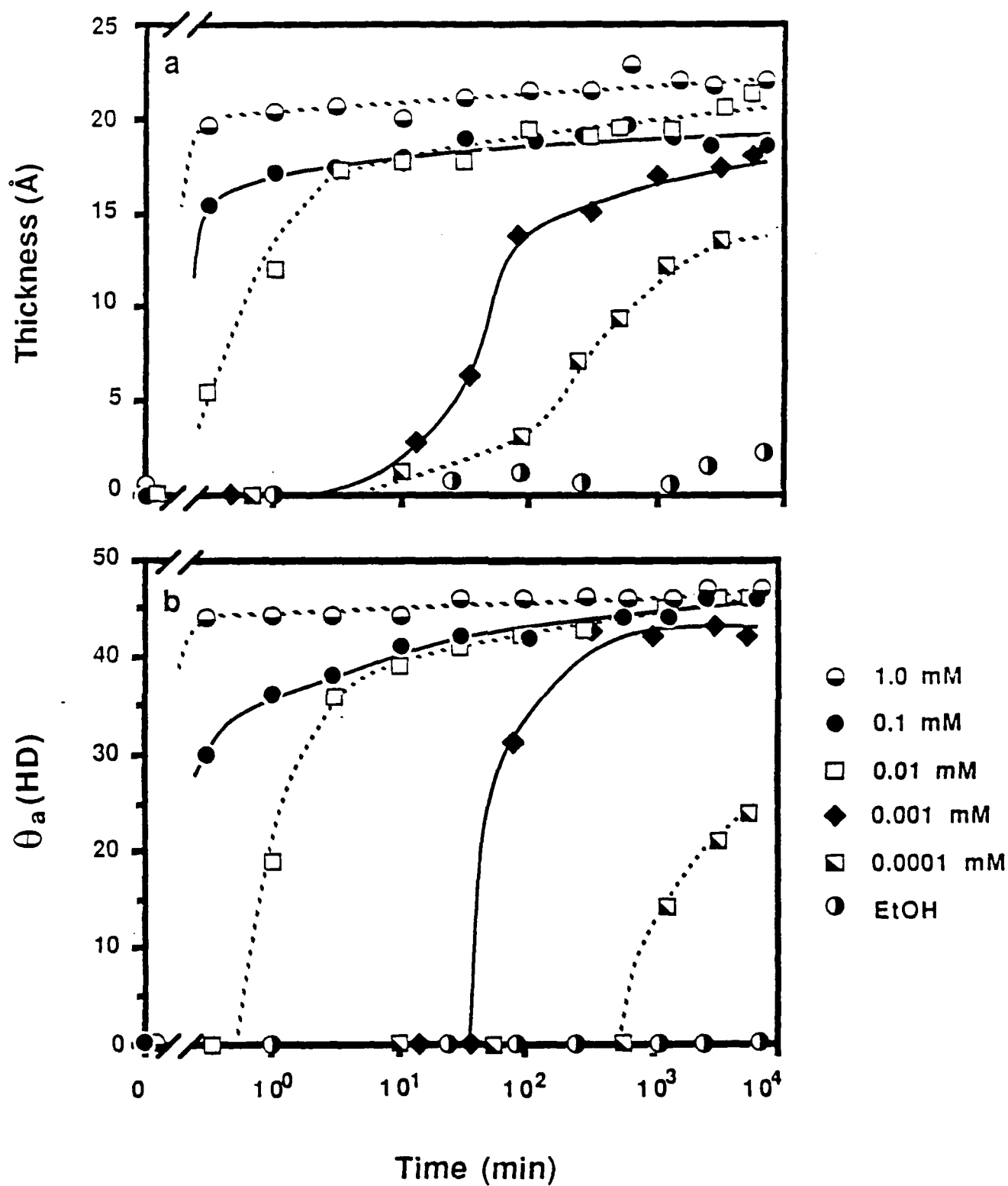


Figure 9. Kinetics of adsorption of octadecanethiol from ethanol as a function of concentration: (a) ellipsometric thickness (b) advancing contact angle of hexadecane (HD). EtOH (\odot) indicates pure ethanol containing no thiol.

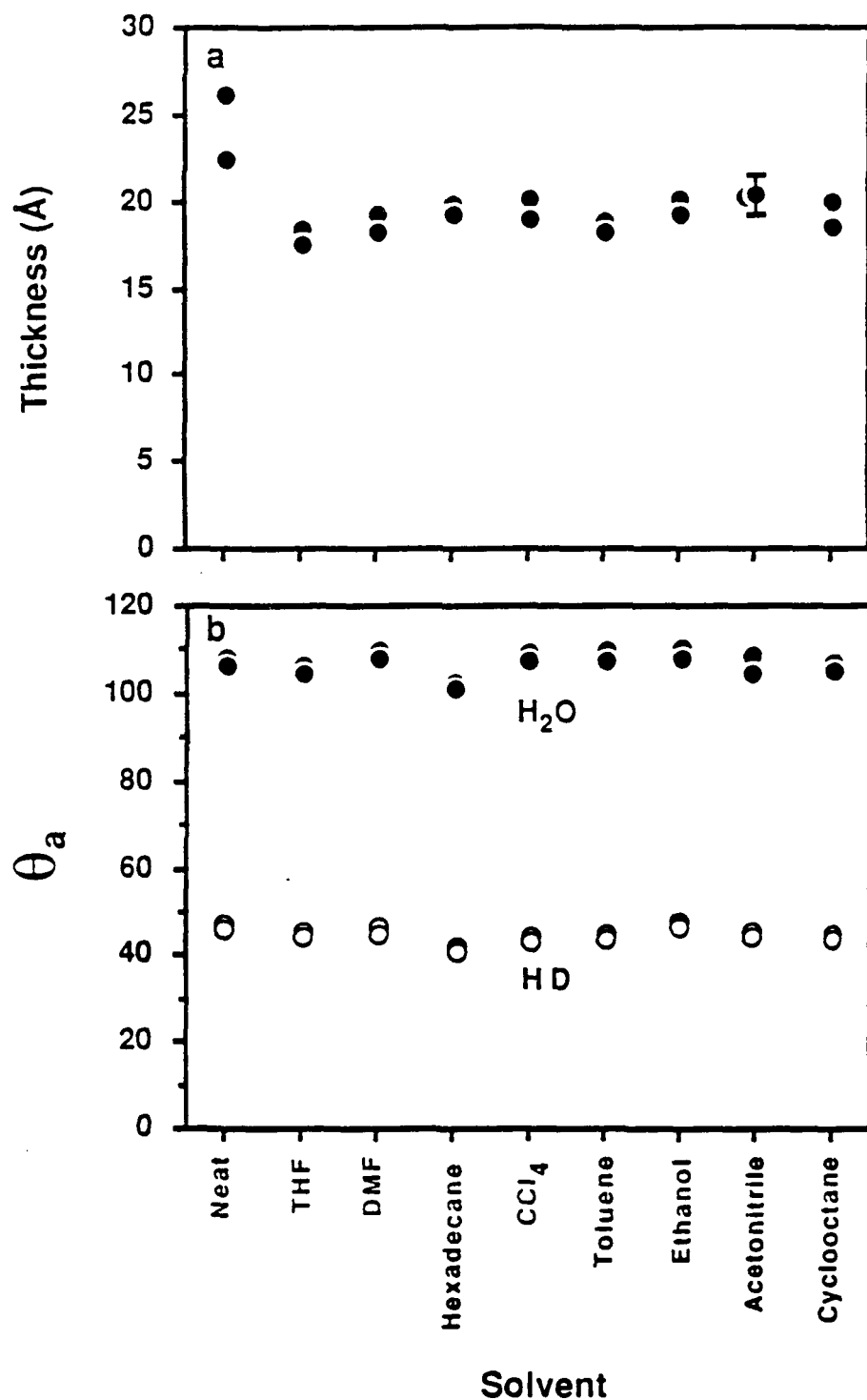


Figure 10. Effect of solvent on formation of hexadecanethiol monolayers. Slides were immersed overnight in 1 mM solutions at room temperature. (a) Ellipsometric thickness. The error bar indicates the range of values found upon repeated measurement of a single gold slide. (b) Advancing contact angles (Method A): (●) water, (○) hexadecane.

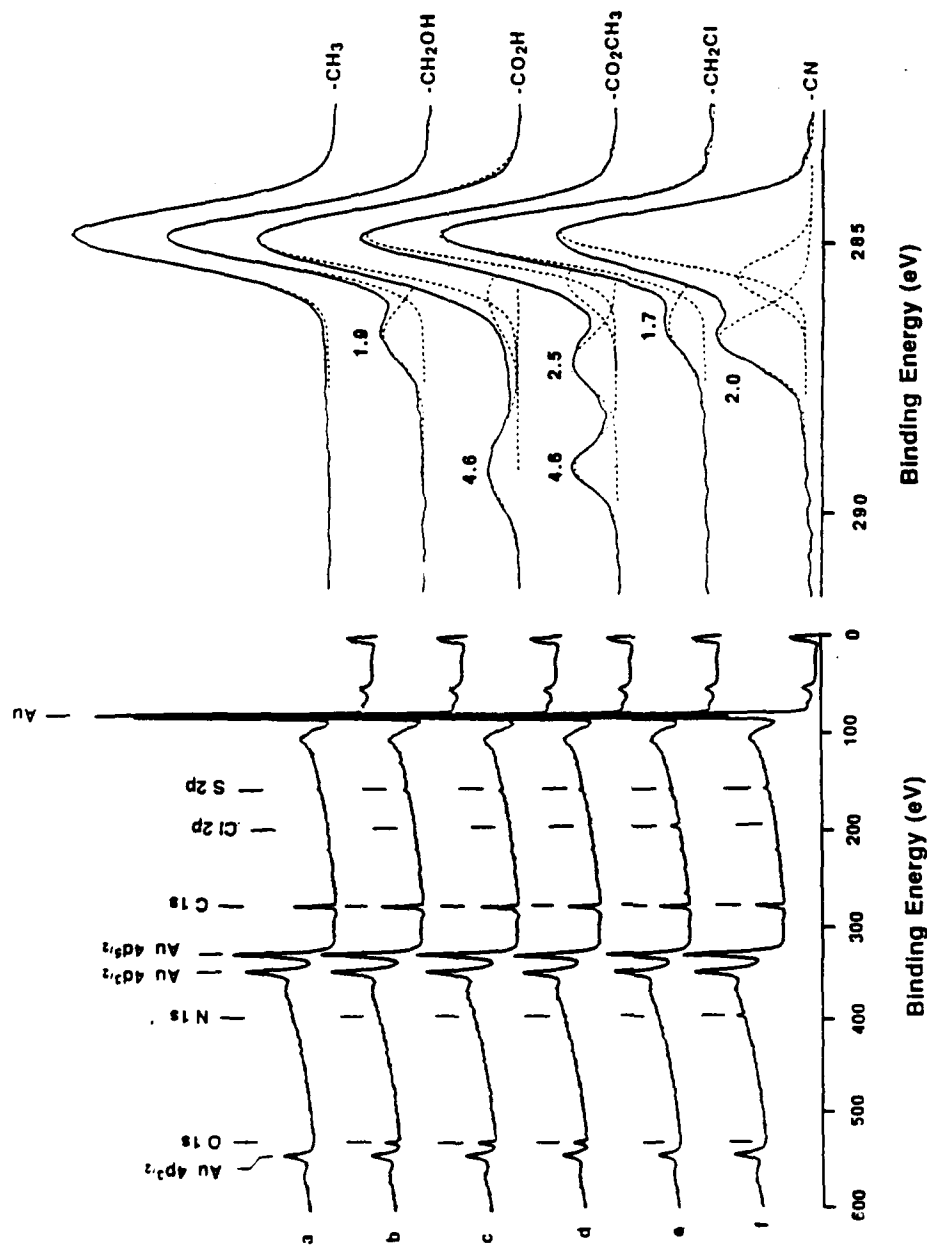


Figure 11. XPS of thiol monolayers on gold: survey spectra (left)

and high resolution spectra of the carbon 1s region (right).

Dotted lines represent computer-generated peak fits using 90%

Gaussian/10% Lorentzian peak shapes. Numbers above the peaks

indicate shifts in binding energy from the principal methylene

peak. (a) HS(CH₂)₁₀CH₃ (b) HS(CH₂)₁₀CH₂OH (c) HS(CH₂)₁₀CO₂H (d)

HS(CH₂)₁₀CO₂CH₃ (e) HS(CH₂)₁₀CH₂Cl (f) HS(CH₂)₁₀CN

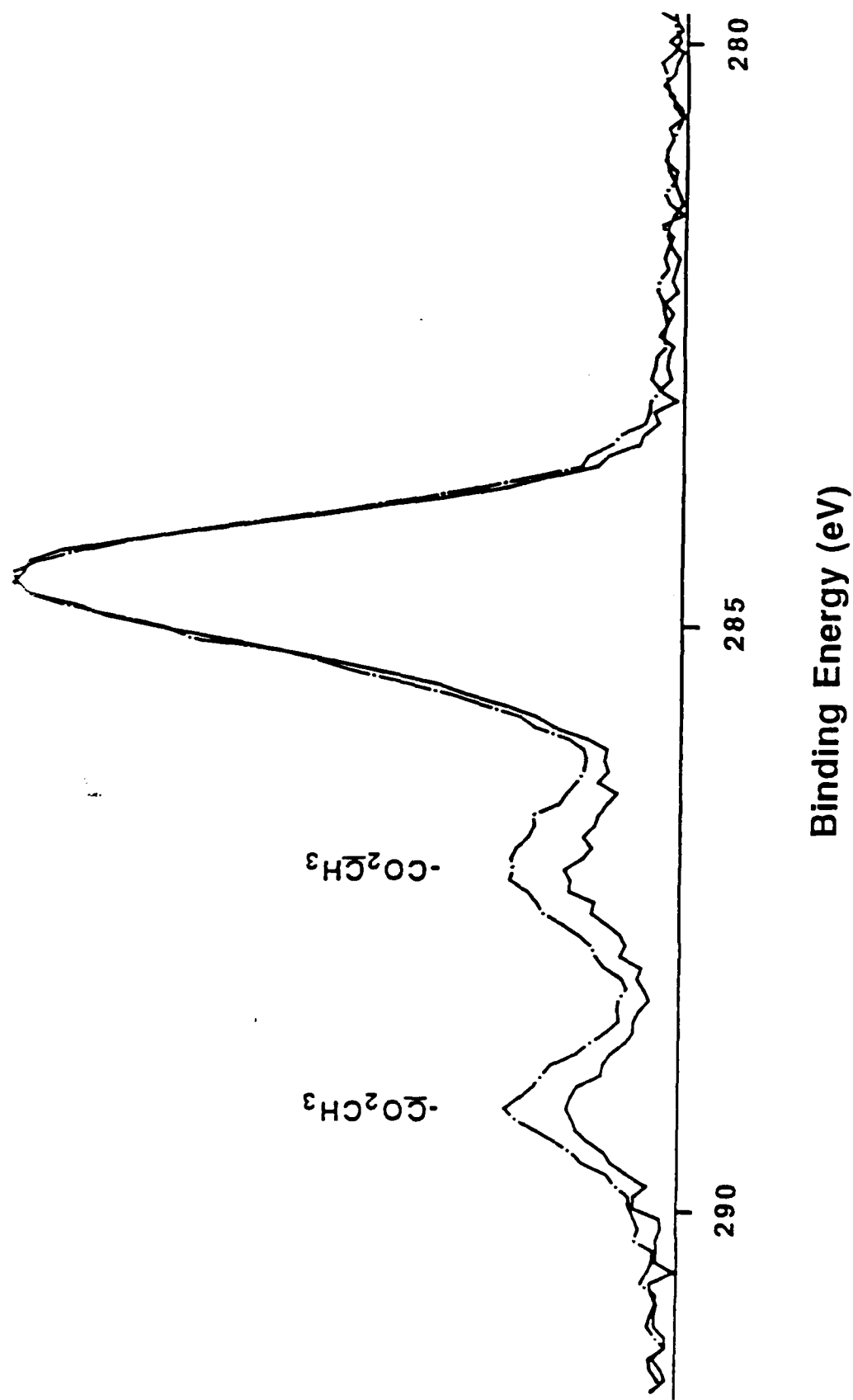


Figure 12. Angle-dependent XPS of the carbon 1s region of a monolayer of $\text{HS}(\text{CH}_2)_{10}\text{CO}_2\text{CH}_3$ adsorbed on gold. Take-off angles of 90° (solid line) and 15° (broken line) are shown.

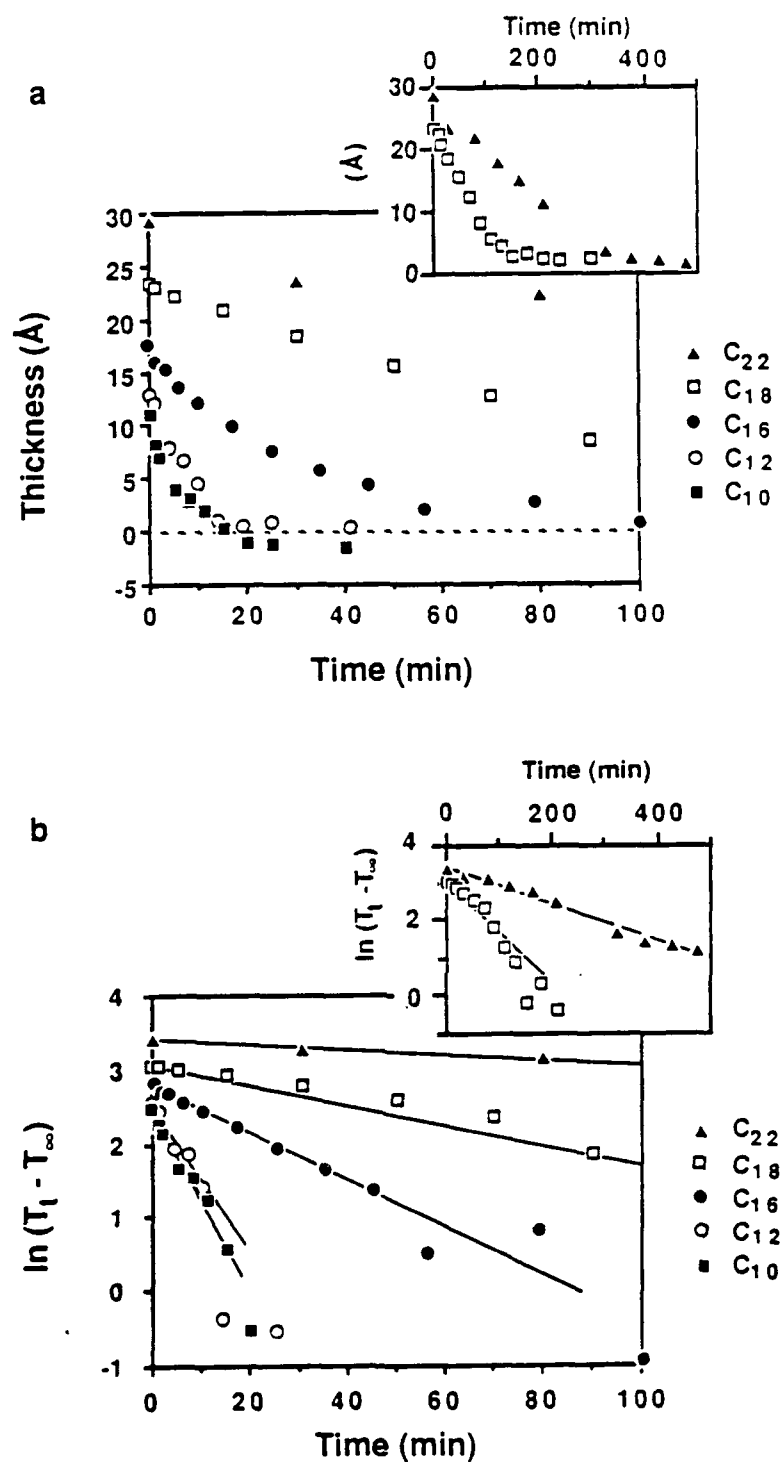


Figure 13. Thermal desorption of monolayers of thiols on gold in contact with hexadecane at 83 °C. (▲) docosanethiol, (◻) octadecanethiol, (●) hexadecanethiol, (○) dodecanethiol, (■) decanethiol. (a) Ellipsometric thickness; inset shows complete desorption profiles for the two longest chain thiols. (b) First-order plot of the corrected thicknesses against time. $T_t - T_\infty$ represents the difference in ellipsometric thickness between time t and long times. Solid lines are linear fits to data points with $T_t - T_\infty > 3$ Å.

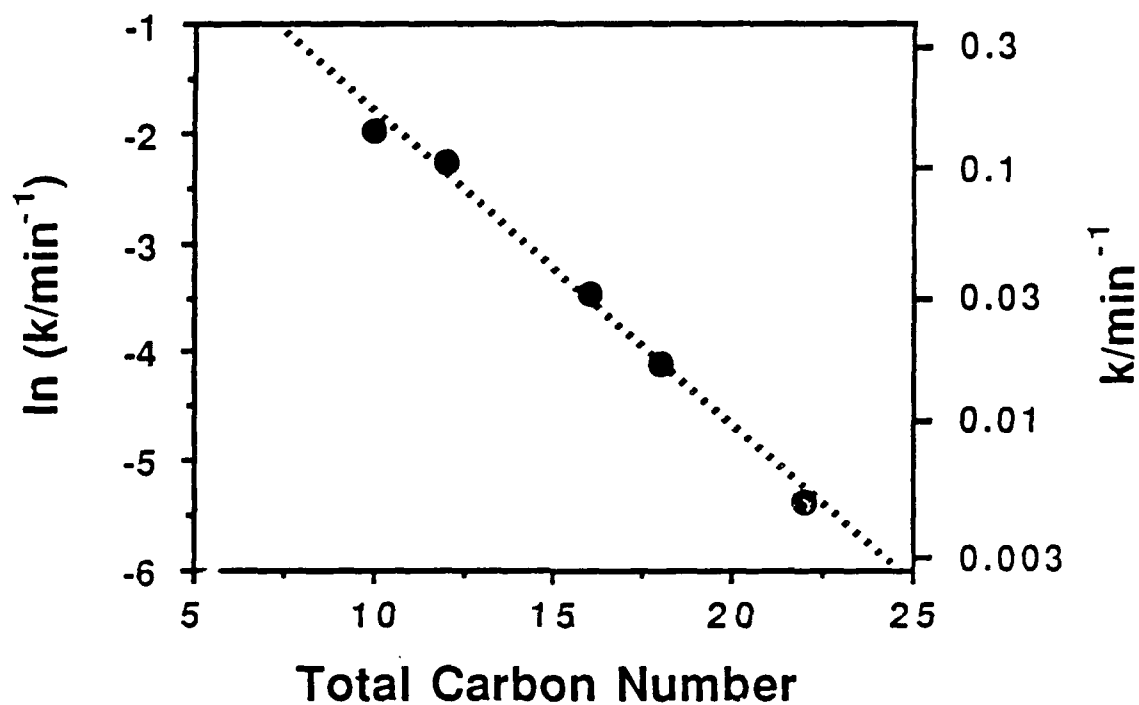


Figure 14. Logarithmic plot of the first-order rate constants for the thermal desorption of thiols from gold in hexadecane at 83 °C. The slope yields a change in activation energy for desorption of 0.2 kcal/mol of methylene groups.

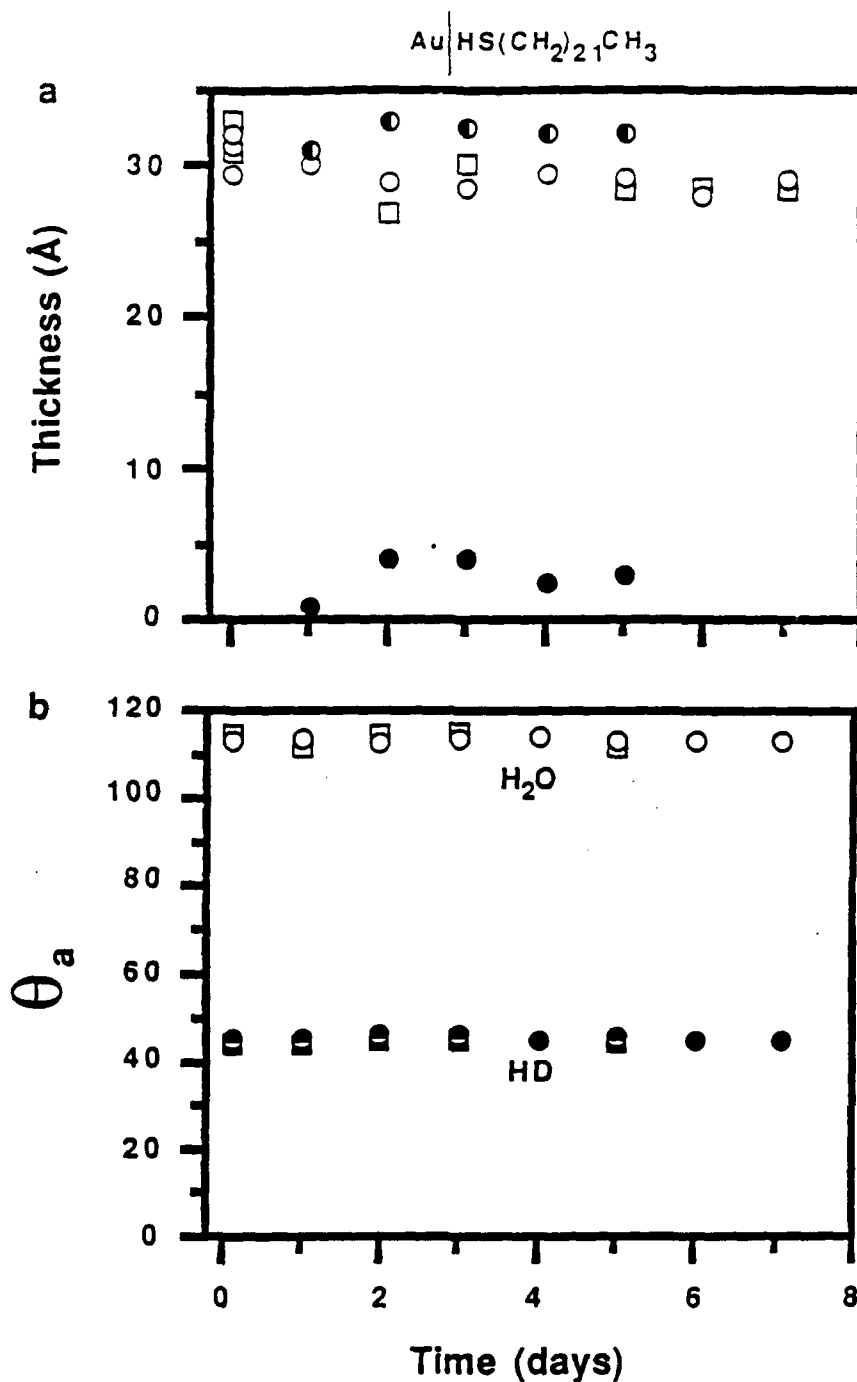


Figure 15. Effect of contamination of gold on ellipsometric thickness (a) and contact angle (b). Squares and circles represent two separate experiments. The abscissa represents the time of storage between the evaporation of the gold and monolayer formation. Ellipsometric thickness was calculated using constants determined immediately prior to immersion in the adsorbate solution (O□) and using initial bare substrate readings obtained shortly after evaporation (O○). The solid symbols (●) indicate the thickness of accumulated contaminants.

CONTRACT NUMBER: N00014-05-A-0098
ATTACHMENT NO.: 1

CONTRACT DATA REQUIREMENTS LIST
INSTRUCTIONS FOR DISTRIBUTION
ARPA/CNR

MINIMUM DISTRIBUTION OF TECHNICAL REPORTS

<u>ADDRESSEE</u>	<u>DODAAD CODE</u>	<u>NUMBER OF COPIES</u>	
		<u>UNCLASSIFIED/UNLIMITED</u>	<u>UNCLASSIFIED/LIMITED AND CLASSIFIED</u>
Director, Advanced Research Projects Agency 1400 Wilson Boulevard Arlington, Virginia 22209 ATTN: Program Management	EX1241	2	2
Scientific Officer	N00014	3	3
Administrative Contracting Officer	N66016	1	1
Director, Naval Research Laboratory, ATTN: Code 2627 Washington, D. C. 20375	N00173	6	1
Defense Technical Information Center Bldg. 3, Cameron Station Alexandria, Virginia 22314	S47031	12	2

One (1) copy of each technical report resulting from work performed in the area of tactical technology shall be sent to:

<u>TACTEC</u>	<u>DODAAD CODE</u>
Battelle Memorial Institute	79986
505 King Avenue	
Columbus, Ohio 43201	

MINIMUM DISTRIBUTION OF REPORTS WHICH ARE NOT TECHNICAL REPORTS

<u>ADDRESSEE</u>	<u>DODAAD CODE</u>	<u>NUMBER OF COPIES</u>	
		<u>UNCLASSIFIED/UNLIMITED</u>	<u>UNCLASSIFIED/LIMITED AND CLASSIFIED</u>
Director, Advanced Research Projects Agency 1400 Wilson Boulevard Arlington, Virginia 22209 ATTN: Program Management	EX1241	2	2
Scientific Officer	N00014	3	3
Administrative Contracting Officer	N66016	1	1

If the Scientific Officer directs, the Contractor shall make additional distribution of technical reports and such other reports as may be specified by the Scientific Officer in accordance with a supplemental distribution list provided by the Scientific Officer.

ABSTRACTS DISTRIBUTION LIST, 3568

Professor T. Marks
Department of Chemistry
Northwestern University
Evanston, Illinois 60201

Dr. Kurt Baum
Fluorochem, Inc.
680 S. Ayon Avenue
Azusa, California 91702

Dr. Ulrich W. Suter
Department of Chemical and Engineering
Massachusetts Institute of Technologies
Room E19-628
Cambridge, MA 02139-4309

Dr. William Bailey
Department of Chemistry
University of Maryland
College Park, Maryland 20742

Dr. J.C.H. Chien
Department of Polymer Science and
Engineering
University of Massachusetts
Amherst, MA 01003

~~Professor G. Whitesides
Department of Chemistry
Harvard University
Cambridge, Massachusetts 02138~~

Dr. K. Paciorek
Ultrasystems, Inc.
P.O. Box 19605
Irvine, California 92715

Dr. Ronald Archer
Department of Chemistry
University of Massachusetts
Amherst, Massachusetts 01002

Professor D. Seyferth
Department of Chemistry
Massachusetts Institute of Technology
Cambridge, Massachusetts 02139

Professor J. Moore
Department of Chemistry
Rensselaer Polytechnic Institute
Troy, New York 12181

Dr. V. Percec
Department of Macromolecular
Science
Case Western Reserve University
Cleveland, Ohio 44106

Dr. Gregory Girolami
Department of Chemistry
University of Illinois
Urbana-Champaign, IL 61801

Dr. Ted Walton
Chemistry Division
Code 6120
Naval Research Lab
Washington D.C. 20375-5000

Professor Warren T. Ford
Department of Chemistry
Oklahoma State University
Stillwater, OK 74078

Professor H. K. Hall, Jr.
Department of Chemistry
The University Arizona
Tucson, Arizona 85721

Dr. Fred Wudl
Department of Chemistry
University of California
Santa Barbara, CA 93106

Professor Kris Matjaszewski
Department of Chemistry
Carnegie-Mellon University
4400 Fifth Avenue
Pittsburgh, PA 15213

Professor Richard Schrock
Department of Chemistry
Massachusetts Institute of Technology
Cambridge, MA 02139

ABSTRACTS DISTRIBUTION LIST, 3568

Professor A. G. MacDiarmid
Department of Chemistry
University of Pennsylvania
Philadelphia, Pennsylvania 19174

Dr. E. Fischer, Code 2853
Naval Ship Research and
Development Center
Annapolis, Maryland 21402

Professor H. Allcock
Department of Chemistry
Pennsylvania State University
University Park, Pennsylvania 16802

Professor R. Lenz
Department of Chemistry
University of Massachusetts
Amherst, Massachusetts 01002

Professor G. Wnek
Department of Chemistry
Rensselaer Polytechnic Institute
Troy, NY 12181

Professor C. Allen
Department of Chemistry
University of Vermont
Burlington, Vermont 05401

Dr. Ivan Caplan
DTNSRDC
Code 0125
Annapolis, MD 21401

Dr. R. Miller
Almaden Research Center
650 Harry Road K918801
San Jose, CA 95120

Dr. William B. Moniz
Chemistry Division
Naval Research Laboratory
Washington, D.C. 20375-5000

Dr. Richard M. Laine
SRI International
333 Ravenswood Avenue
Menlo Park, California 94025

Dr. L. Buckley
Naval Air Development Center
Code 6063
Warminster, Pennsylvania 18974

Dr. James McGrath
Department of Chemistry
Virginia Polytechnic Institute
Blacksburg, Virginia 24061

Dr. Geoffrey Lindsay
Chemistry Division
Naval Weapons Center
China Lake, California 93555

Professor J. Salamone
Department of Chemistry
University of Lowell
Lowell, Massachusetts 01854

Dr. J. Griffith
Naval Research Laboratory
Chemistry Section, Code 6120
Washington, D. C. 20375-5000

Professor T. Katz
Department of Chemistry
Columbia University
New York, New York 10027

Dr. Christopher K. Ober
Department of Materials Science
and Engineering
Cornell University
Ithaca, New York 14853-1501